J. Fluid Mech. (1987), *vol.* 174, *pp.* 81–112
Printed in Great Britain

The rapid expansion of a supersonic turbulent flow: role of bulk dilatation

By J. P. DUSSAUGE AND J. GAVIGLIO
Institut de Mécanique Statistique de la Turbulence, LA CNRS No. 130, Université d'Aix-Marseille II, France

(Received 9 February 1985 and in revised form 27 May 1986)

The rapid expansion of a turbulent boundary layer in supersonic flow is studied analytically and experimentally. Emphasis is placed on the effect of bulk dilatation on turbulent fluctuations. The hypotheses made in the analysis are similar to those in the rapid distortion theory and are used to simplify second-order closures. By assuming that the fluctuating velocity is solenoidal an extension of classical subsonic models is proposed. A new variable is defined, which takes into account the mean density variations, and behaves like the Reynolds stress tensor in subsonic flows with weak inhomogeneities and a weak dissipation rate. The results of the analysis are compared with turbulence measurements performed in a supersonic boundary layer subjected to an expansion fan. The proposed approximations describe correctly the evolution of turbulence intensities: bulk dilatation contributes predominantly to the Reynolds stress evolution. The boundary layer is 'relaminarized' by the expansion. Downstream of the latter, the layer returns to equilibrium. Measurements show that the turbulence decays slowly in the outer layer and increases rapidly in the inner layer.

1. Introduction

The initial work on turbulence in compressible fluids (Kovasznay 1953; Moyal 1952; Morkovin 1962) served to clarify the similarities and differences that exist between low- and high-speed fluid flow. The analysis of experimental results led Morkovin (1962) to expect 'that the essential dynamics of these supersonic shear flows will follow the incompressible pattern'. Compressibility, therefore, seems to have little effect on the turbulence structure, if the flow is non-hypersonic (Bradshaw 1977). Recent space–time correlation measurements (Demetriades 1976; Bonnet & Alziary de Roquefort 1982) reinforced these conclusion. However, the flows considered by these investigators were quasi-parallel, with slow longitudinal evolution and no heat source. In such conditions, the mean velocity field can be described as a nearly pure shear flow and the mean velocity divergence is small and can be neglected; although the mean density varies in the direction perpendicular to the wall, there is practically no mean compressibility since the mean velocity field is nearly solenoidal. Moreover, since the fluctuating Mach number has low subsonic values, it is not surprising that these flows exhibited properties roughly like those found in low-speed flows.

In contrast, if a supersonic turbulent flow is subjected to a strong pressure gradient, the results demonstrate some surprising responses. Longitudinal mean density variations are created, the mean velocity divergence can become comparable to the mean shear, and the turbulent transport can be strongly affected through the 'extra rate of strain' terms in the kinetic energy and Reynolds stress equations. Some

aspects of this problem were examined by Batchelor (1955), and the implications for turbulence models were considered by Wilcox & Alber (1972), Bradshaw (1974) and Rubesin (1976). However, as noted by Bradshaw (1976), little is known about the influence of bulk dilatation on the turbulence structure.

Another problem typical of high-speed flows is to determine how the turbulent fields are affected by density fluctuations. The density fluctuations appear explicitly in the equations for the turbulent kinetic energy and the Reynolds stress tensor when there is a pressure gradient; these terms can be important if the pressure gradient is strong enough (Gaviglio *et al.* 1977). Therefore, if it is assumed that in a zero-pressure-gradient non-hypersonic flow the turbulence structure is similar to that observed in subsonic flows, an indication of the influence of density fluctuations in the accelerated zone can be obtained.

In the present work (Dussauge 1981), we attempt to improve our understanding of these phenomena by both analytical and experimental means. The analysis (§§2) deals mainly with the changes in the turbulent transfer induced by a mean dilatation, that is, the action of the mean field on the turbulence structure. The simplest case occurs when the distortion is very rapid; this situation is considered here. As will be seen in §2, the rapid distortion theory has been developed to the extent that it is able to predict the evolution of turbulent quantities in various situations. For example, an adaptation of this theory to the case of supersonic flows has been proposed by Goldstein (1978) and was applied to predict the evolution of turbulence in a Prandtl–Meyer expansion. However, this work supposes that the mean field is irrotational and homentropic and the incident turbulent field is isotropic. If we now consider rapidly distorted shear flows, the mean field is vortical, there are entropy gradients and the initial turbulent field is anisotropic. In this case, it is difficult to apply Goldstein's results directly. In the present work, the basic assumptions of the rapid distortion theory are used to simplify second-order closures. The analysis shows that classical incompressible models for the rapid part of the pressure velocity correlation can be extended to compressible flow. Calculations are made and compared with experimental results. The experiment is presented (§§3 and 4): measurements are performed in a boundary layer subjected to a rapid expansion with a significant decrease in mean density and pressure. It is well known that these conditions cause the turbulence level to decrease, and if the pressure change is large enough a 'relaminarization' or 'reverse transition' can occur (Sternberg 1954; Morkovin 1955; Narasimha & Sreenivasan 1979). However, the mechanism leading to this relaminarization in supersonic flows was not clearly identified, although Bradshaw (1976) suggested that bulk dilatation could play an important role. The experimental results include measurements of mean and fluctuating quantities in the expansion itself and in the relaminarized boundary layer recovering to new equilibrium properties. Finally (§5), the comparison between analytical and experimental results is discussed.

2. Analysis

2.1. *Preliminaries: the assumption concerning the velocity fluctuation field*

We wish to describe the rapid distortion of a turbulent velocity field by a bulk dilatation, that is, by a mean field where the velocity gradient $\partial\tilde{u}_i/\partial x_j$ reduces to $\frac{1}{3}\,\partial\tilde{u}_k/\partial x_k\delta_{ij}$ ($\tilde{u}_k$ is the component of the mean mass-weighted velocity and δ_{ij} is the Kronecker delta). Classically, the equations are obtained by linearizing the momentum equation, taking the Fourier transform and calculating the three-dimensional spectra related to Reynolds stresses (see for example Batchelor & Proudman 1954; Ribner

& Tucker 1952; Craya 1958; Moffatt 1968; Hunt 1977; Goldstein 1979; Townsend 1980). After integrating in wavenumber space, the turbulent kinetic energy or the shear stresses are deduced. Earlier versions of this theory used the assumption of local homogeneity, i.e. the turbulent integral scale was supposed small compared with the spatial scale of the mean flow. This difficulty is overcome in more recent versions (Hunt 1973, 1977). Indeed, the local homogeneity assumption is required to obtain solutions of an analytical form in simple situations. This assumption is however independent of the basic idea that the problem is governed by a linear set of equations, if small-amplitude fluctuations are subjected to a mean distortion during a time much shorter than a characteristic timescale of the eddies. With such a method, the initial three-dimensional spectra must be specified. Unfortunately, the latter are not generally known when the flow upstream is a shear flow. Moreover, the experimental comparisons usually involve only one of the Reynolds stresses, i.e. the variance of longitudinal velocity fluctuations; in supersonic flows this quantity can be more accurately measured than the full turbulent kinetic energy or the associated spectra. Hence we consider the Reynolds stress evolution, rather than the evolution of other quantities. The simplifications of second-order closure needed for a rapid distortion approximation are not straightforward, as pointed out by Hunt (1977), mainly because terms involving pressure fluctuations must be modelled. Because of this requirement, the solution is generally not exact. By examining the pressure equation, however, some trends may be found, and these may be used to get information regarding the Reynolds stress evolution.

Another difficulty encountered at the outset is to define the properties of the velocity fluctuation field in a supersonic shear flow: this is required to describe the pressure fluctuations, which in turn influence the turbulent transfer process.

It was noted in the introduction that, for zero-pressure-gradient flows, the fluctuating motions in subsonic and supersonic flows seem to have common statistical properties. This was recently confirmed by the direct simulations of compressible turbulence by Feiereisen, Reynolds & Ferziger (1981). Their results suggest that in a homogeneous shear flow the compressible (non-zero divergence) part of the fluctuating motion can be neglected if the fluctuating Mach number is sufficiently small. Moreover, supersonic boundary layers in a moderate pressure gradient can be successfully computed with the same methods used in subsonic flows (see, for instance, Bradshaw 1974; Wilcox & Rubesin 1980; Galmes, Dussauge & Dekeyser 1983), suggesting that the turbulent mixing process is governed by similar mechanisms. Hence the assumption that the fluctuating motion is incompressible, i.e. $\partial u_i'/\partial x_i = 0$, appears to be a reasonable approximation. This assumption is not new. For example, Ribner & Tucker (1952) used it to calculate the damping of turbulence through nozzles; the results yield the right trend, even in shear flows (Sternberg 1954; Morkovin 1955). Later work by Goldstein (1978), however, showed that in an irrotational distortion the fluctuating field does not remain truly solenoidal. Nevertheless, we shall assume here that, to a good approximation, the fluctuating field is solenoidal. With respect to Moyal's separation (1952) of the velocity fluctuation into a solenoidal part and a non-zero-divergence part, we restrict our analysis to situations where the solenoidal part is much larger than the other part. It then follows that material derivatives of entropy, and pressure fluctuations (but not necessarily the fluctuations themselves) are small, as required by mass conservation. This choice implies that the phenomenology used in a incompressible turbulence can be applied, and therefore the turbulent scales can be derived from subsonic work.

Favre averaged variables are used in the present work. The velocity fluctuation u_i' is not centred since $\overline{u_i'} \neq 0$; then it is clear that the condition $\partial u_i'/\partial x_i = 0$ is not fulfilled

in the general case. It would probably be more convenient to use the hypothesis:

$$\partial u_i'^{\mathrm{R}}/\partial x_i = \partial(u_i' + \overline{\rho' u_i'}/\bar{\rho})/\partial x_i = 0,$$

where $u_i'^{\mathrm{R}}$ denotes the velocity fluctuation in Reynolds averaging. However, in our particular case, only small fluctuations will be considered; therefore, $\overline{\rho' u_i'}/\bar{\rho}$ is much smaller than u_i' and the two definitions of velocity fluctuation can be interchanged with very little error.

2.2. *Order of magnitude analysis*

Here, we determine the order of magnitude of terms involving density or temperature fluctuations.

As recalled by Bradshaw (1977) and Fernholz & Finley (1981), the 'Strong Reynolds Analogy' (Morkovin 1962; Young 1951) holds for flows without heat sources. That is,

$$\frac{(\overline{T'^2})^2}{\bar{T}} = \frac{(\overline{\rho'^2})^2}{\bar{\rho}} = (\gamma-1)M^2 \frac{(\overline{u_1'^2})^2}{\tilde{u}_1}. \tag{1}$$

Here, T represents the temperature, ρ the density, γ the ratio of specific heats, M the Mach number, u_1 the longitudinal velocity component, $(\bar{})$ an ensemble average, $(\tilde{})$ a mass weighted average and $(\ )'$ a fluctuation, Equation (1) has been found to apply in some complex supersonic flows (Gaviglio *et al.* 1977; Debieve 1983) and it will be verified experimentally in the present experiment.

Since the Prandtl number for air is nearly unity, it will be assumed that the temperature and velocity fluctuations have approximately the same spatial scales.

Consider a rapid distortion. Here, the time of flight of a fluid particle through the region of distortion is small compared to the timescale of the energetic motions. The latter is of the same order as the 'turnover time' of the large structures, and therefore approximately equal to Λ/q', where Λ represents an integral lengthscale deduced for example from the longitudinal velocity correlation and q' is given by the relation $q'^2 = \widetilde{u_i' u_i'}$ (Sabot, Renault & Comte-Bellot 1973). If U is an average value of the mean velocity in the distortion, the length of which is L_{d}, we obtain the classical inequality.

$$\frac{q'}{U}\frac{L_{\mathrm{d}}}{\Lambda} \ll 1. \tag{2}$$

If condition (2) is fulfilled, it may be assumed that the kinetic energy dissipation rate per unit mass ϵ does not vary significantly in the distortion, and the distortion is considered to be 'rapid'.

The Reynolds stress equations, written in terms of mass weighted variables, are given by:

$$\left.\begin{aligned}
\frac{\mathrm{D}}{\mathrm{D}t}\widetilde{u_i' u_j'} = &-\widetilde{u_i' u_k'}\frac{\partial \tilde{u}_j}{x_k} - \widetilde{u_j' u_k'}\frac{\partial \tilde{u}_j}{x_k} \quad \text{(I)},\\
&+\frac{\overline{\rho' u_i'}}{\bar{\rho}^2}\frac{\partial \bar{p}}{\partial x_j} + \frac{\overline{\rho' u_j'}}{\bar{\rho}^2}\frac{\partial \bar{p}}{\partial x_i} \quad \text{(II)},\\
&-\frac{1}{\bar{\rho}}\left(\overline{u_i'\frac{\partial p'}{\partial x_j}} + \overline{u_j'\frac{\partial p'}{\partial x_j}}\right) \quad \text{(III)},\\
&-\frac{1}{\bar{\rho}}\frac{\partial}{\partial x_k}(\overline{\rho u_i' u_j' u_k'} - \overline{f_{ik} u_j'} - \overline{f_{jk} u_i'}) \quad \text{(IV)},\\
&-\epsilon_{ij} \quad \text{(V)}.
\end{aligned}\right\} \tag{3}$$

(Favre *et al.* 1976).

The turbulent stress $\widetilde{u_i'u_j'}$ is defined by $\widetilde{u_i'u_j'} = \overline{\rho u_i'u_j'}/\bar{\rho}$. In this equation, $\partial/\partial x_k$ is the space derivative in the k direction; $\mathrm{D}/\mathrm{D}t = (\partial/\partial t) + \tilde{u}_k(\partial/\partial x_k)$ is the derivative along a mean streamline; p is the pressure; f_{ik} the viscous stress and ϵ_{ij} the dissipation rate of $\widetilde{u_i'u_j'}$.

Terms (I) and (II) are production terms and terms (IV) and (V) represent the diffusive and dissipative effects, respectively. When the flow is strongly accelerated, the significant contributions to the first production term are those involving $\partial\tilde{u}_1/\partial x_1$, and $\partial\tilde{u}_1/\partial x_1 \sim \Delta U/L_\mathrm{d}$, where ΔU is the velocity increase through the distortion. The longitudinal pressure gradient is given approximately by $\partial\bar{p}/\partial x_1 \sim \rho U \Delta U/L_\mathrm{d}$; the transverse pressure gradient is assumed to be comparable to $\partial\bar{p}/\partial x_1$.

The $\overline{\rho' u_i'}$ contribution in the second production term is obtained by assuming that the density–velocity correlation coefficient is nearly 1, and by using (1). The dissipation rate ϵ_{ij} is determined by assuming that isotropy is achieved in the dissipative range, and by the classical inviscid estimate $\epsilon \sim q'^3/\Lambda$.

The diffusion terms are a little more difficult to deal with since they depend on both the turbulent quantities and the density variation; these various contributions are tentatively taken into account in Appendix A, where further details of the order of magnitude estimates are reported.

From these estimates, we find that for moderate supersonic Mach numbers, terms (I) and (II) have comparable values (Gaviglio *et al.* 1977), and the dissipation and diffusion are small compared to the production if the following inequalities hold:

$$\frac{q'}{\Delta U}\frac{L_\mathrm{d}}{\Lambda} \ll 1, \tag{4}$$

$$\frac{q'}{\Delta U}\frac{\Delta\rho}{\rho} \ll 1, \tag{5a}$$

$$\frac{q'}{\Delta U} \ll 1. \tag{5b}$$

Inequality (4) represents the condition that dissipation can be neglected and inequalities (5*a*) and (5*b*) hold if the diffusion is small (see Appendix A).

We need to pay particular attention to the pressure terms (term III in (3)). In many subsonic second-order models, these terms are separated into two parts: a 'rapid' part, corresponding to the pressure fluctuation developed in a rapid distortion, and a 'return-to-isotropy' part, corresponding to the non-linear terms of the pressure equation. If the latter have the same order of magnitude in supersonic and subsonic flows, a rough estimate can be given by $\epsilon(\widetilde{u_i'u_j'}/q'^2 - \frac{1}{3}\delta_{ij})$. At worst, the 'return-to-isotropy' terms are probably as large as ϵ and therefore, if inequality (4) holds, the return-to-isotropy term can be neglected.

2.3. *The rapid part of the pressure–strain term and the effects of mean dilatation*

The so-called 'rapid part' of the pressure term is obtained by linearizing the Euler equation for small fluctuations. The approach given here, developed in Dussauge (1981), is basically adapted from Lumley (1975). If $\partial u_i'/\partial x_i = 0$, and if the mean flow is steady with small mean velocity second derivatives, the pressure equation is then given by

$$-\frac{\partial^2 p'}{\partial x_k \partial x_k} + \frac{1}{\bar{\rho}}\frac{\partial\bar{\rho}}{\partial x_i}\frac{\partial p'}{\partial x_i} = 2\bar{\rho}\frac{\partial u_i'}{\partial x_j}\frac{\partial\tilde{u}_j}{\partial x_i} + \frac{\partial\rho'}{\partial x_i}\tilde{u}_j\frac{\partial\tilde{u}_i}{\partial x_j} + \rho'\left(\frac{\partial\tilde{u}_i}{\partial x_j}\frac{\partial\tilde{u}_j}{\partial x_i} - \frac{1}{\bar{\rho}}\frac{\partial\bar{\rho}}{\partial x_i}\tilde{u}_j\frac{\partial\tilde{u}_i}{\partial x_j}\right). \tag{6}$$

The first term on the right-hand side is the same as that found in subsonic flows and the second one is formally analogous to the leading term in buoyancy problems. It can be shown (see Appendix B) that in our case these two terms are of the same order. In addition, it can be seen that compressibility introduces two supplementary terms: the second term on the left-hand side and the last term on the right-hand side. Note that, on the left-hand side, the term $(\partial(\ln\bar{\rho})/\partial x_i)\,(\partial p'/\partial x_i)$ involves fluctuations at lower wavenumbers than the Laplacian term does. Hence, we can find a limiting wavenumber where only $\partial^2 p'/\partial x_k \partial x_k$ needs to be retained. An estimate of this limit, given in Appendix B, indicates that the wavenumber k must satisfy the condition

$$k \gg \frac{\Delta\rho}{\rho}\frac{1}{L_\mathrm{d}}.$$

Alternatively, using Taylor's hypothesis, a condition on frequency n can be obtained

$$n \gg \frac{U}{2\pi}\frac{\Delta\rho}{\rho}\cdot\frac{1}{L_\mathrm{d}}. \tag{7}$$

It is also shown in Appendix B that the terms in the brackets on the right-hand side can be neglected if

$$n \gg \frac{\Delta U}{L_\mathrm{d} 2\pi}. \tag{8}$$

In our experiment, the inequalities (7) and (8) are satisfied at all but the lowest frequencies. Poisson's equation can be used for the main part of the energetic range, as long as we exclude the lowest wavenumbers. Hence (6) reduces to

$$-\frac{\partial^2 p'}{\partial x_k \partial x_k} = 2\bar{\rho}\frac{\partial u_i'}{\partial x_j}\frac{\partial \tilde{u}_j}{\partial x_i} + \frac{\partial \rho'}{\partial x_i}\tilde{u}_j\frac{\partial \tilde{u}_i}{\partial x_j}. \tag{9}$$

Since (9) is linear, the contributions of the source terms can be examined separately.

Consider the contribution of u_i' to the pressure fluctuations. For this purpose, it is convenient to separate the velocity gradient tensor into an isotropic part $\frac{1}{3}\,\partial\tilde{u}_k/\partial x_k \delta_{ij}$, a symmetric part with zero trace (pure strain) and an antisymmetric part (vorticity tensor):

$$\frac{\partial u_i'}{\partial x_j} = d_{ij} + r_{ij}\left(\frac{\partial u_k'}{\partial x_k} \text{ is assumed to be zero}\right),$$

$$\frac{\partial \tilde{u}_i}{\partial x_j} = \tfrac{1}{3}\,\partial\tilde{u}_k/\partial x_k \delta_{ij} + D_{ij} + R_{ij},$$

with

$$d_{ii} = r_{ii} = D_{ii} = R_{ii} = 0,$$

$$d_{ij} = d_{ji}, \quad r_{ij} = -r_{ji},$$

$$D_{ij} = D_{ji}, \quad R_{ij} = -R_{ji}.$$

Hence,

$$-\frac{\partial^2 p'}{\partial x_k \partial x_k} = 2\bar{\rho}\,(d_{ij}D_{ij} + r_{ij}R_{ij}). \tag{10}$$

It can be seen from (10) that p' depends only on the deviatoric part of the mean velocity gradient and not on the bulk dilatation. It should be stressed that this result is obtained only because the fluctuating motion was assumed to be incompressible, and the same conclusion can be reached by applying this assumption to the models proposed by Lumley (1975) or Launder, Reece & Rodi (1975) for the incompressible case. Therefore, it can be shown that the rapid part of the pressure-strain term

depends only on the deviatoric part $\partial\tilde{u}_i/\partial x_j - \frac{1}{3}\partial\tilde{u}_k/\partial x_k \delta_{ij}$ and it does not depend on the divergence of the mean velocity field. In fact, the supersonic models are obtained simply by replacing $\partial\tilde{u}_i/\partial x_j$ in the low-speed formulation by $\partial\tilde{u}_i/\partial x_j - \frac{1}{3}(\partial\tilde{u}_k/\partial x_k)\delta_{ij}$.

The particular case of a rapid distortion with only mean dilatation can now be examined. As the fluctuating pressure terms do not depend on mean velocity divergence, (3) reduces to:

$$\frac{\mathrm{D}}{\mathrm{D}t}\widetilde{u_i'u_j'} = -\tfrac{2}{3}\widetilde{u_i'u_j'}\frac{\partial\tilde{u}_k}{\partial x_k}. \tag{11}$$

By using mass conservation, the integration of (11) is straightforward. Hence, $T_{ij} = \widetilde{u_i'u_j'}/(\bar{\rho})^{\frac{2}{3}}$ is constant along a mean streamline whatever i and j; an identical result was found by Batchelor (1955) from dimensional arguments based on angular momentum conservation. If $\widetilde{u_i'u_j'}$ remains proportional to $\bar{\rho}^{\frac{2}{3}}$, whatever i and j, all the turbulent stresses vary at the same relative rate and the anisotropy of the Reynolds stress tensor remains unchanged.

The contribution of ρ' to the pressure fluctuation is now examined. For strongly accelerated inviscid flows, the acceleration vector $\tilde{u}_j(\partial\tilde{u}_i/\partial x_j)$ is virtually balanced by the mean pressure gradient $-(1/\bar{\rho})(\partial\bar{p}/\partial x_i)$. Moreover, if the 'no-sound' assumption $\rho'/\bar{\rho} \approx -T'/\tilde{T}$ (Laufer 1969) can be applied, and if the mean temperature and velocity fields are only weakly inhomogeneous, (9) becomes

$$\frac{\partial^2 p'}{\partial x_k \partial x_k} = -\frac{1}{\tilde{T}}\frac{\partial T'}{\partial x_i}\frac{\partial\bar{p}}{\partial x_i}. \tag{12}$$

According to the same argument, the production terms (II) of (3) can be expressed in another form. These terms can be related to the Reynolds stress through algebraic relationships to avoid modelling the turbulent mass flux by a transport equation. First, the 'no-sound' assumption gives $\overline{\rho' u_i'}/\bar{\rho} = -\overline{T' u_i'}/\tilde{T}$ and term II becomes

$$-\frac{\overline{T'u_i'}}{\tilde{T}\bar{\rho}}\frac{\partial\bar{p}}{\partial x_j} - \frac{\overline{T'u_j'}}{\tilde{T}\bar{\rho}}\frac{\partial\bar{p}}{\partial x_i}.$$

Secondly, the Strong Reynolds Analogy (SRA) leads to the following expressions (Debieve, Gouin & Gaviglio 1982):

$$\frac{\overline{T'u_1'}}{\tilde{T}} \approx -R_{T1}(\gamma-1)M^2\frac{\widetilde{u_1'^2}}{\tilde{u}},$$

$$\frac{\overline{T'u_2'}}{\tilde{T}} \approx -\frac{R_{T2}}{R_{12}}(\gamma-1)M^2\frac{\widetilde{u_1'u_2'}}{\tilde{u}},$$

and $\overline{T'u_3'} = 0$ for a two-dimensional flow.

R_{T1}, R_{T2} are the correlation coefficients between temperature fluctuations and the velocity fluctuation components u_1', u_2', respectively, and R_{12} is the correlation coefficient between u_1' and u_2'; $\tilde{u}$ is the modulus of mean velocity.

Then term II of (3), and (12) have the same form as in buoyancy problems. For example, if $\partial u_i'/\partial x_i = 0$, the model proposed by Lumley (1975) can be applied to our case. The formulation is linear with respect to $\overline{T'u_i'}$, $\widetilde{u_j'u_i'}$ and T_{ij}, and therefore in practical cases T_{ij} is the only variable that appears in the present problem.

Before describing the models used in the calculations, the compressibility effects involved in the present analysis can be considered. For simplicity, the contributions of mean velocity divergence and of pressure gradient are examined separately. However, these two effects could have been studied together by writing the simplified

Reynolds stress equation, assuming that the mean velocity gradient reduces to $\frac{1}{3}(\partial\tilde{u}_k/\partial x_k)\delta_{ig}$ and finally noting that the divergence does not appear in the pressure-strain terms. After some obvious algebraic manipulations the equation for T_{ij} is obtained:

$$\frac{\mathrm{D}}{\mathrm{D}t}T_{ij} = \frac{\overline{\rho' u_j'}\frac{\partial\bar{p}}{\partial x_i} + \overline{\rho' u_i'}\frac{\partial\bar{p}}{\partial x_j}}{\bar{\rho}^{\frac{3}{3}}} + \frac{\overline{u_i'\frac{\partial p'}{\partial x_j}} + \overline{u_j'\frac{\partial p'}{\partial x_i}}}{\bar{\rho}^{\frac{5}{3}}},$$

with

$$\frac{\partial^2 p'}{\partial x_k \partial x_k} \approx -\frac{1}{\bar{T}}\frac{\partial T''}{\partial x_k}\frac{\partial\bar{p}}{\partial x_k} \approx +\frac{1}{\bar{\rho}}\frac{\partial\rho'}{\partial x_k}\frac{\partial\bar{p}}{\partial x_k}.$$

In the present problem the effect of streamwise mean density variations is contained in T_{ij} itself: this is due to the solenoidal velocity fluctuations assumption. The influence of ρ' (or T''), combined with the mean pressure gradient is represented by the terms on the left-hand side of the equation. Then for $\rho'/\bar{\rho} \ll 1$ or for zero mean pressure gradient the only compressibility effect to be taken into account is due to longitudinal changes of mean density. If there is a mean pressure gradient, the density fluctuations will affect T_{ij}. The limitation of the present approach appear more clearly: in a constant pressure quasi-parallel flow, for example a supersonic mixing layer, the longitudinal gradient of mean density is small, so $\partial\tilde{u}_k/\partial x_k$ can probably be neglected in comparison with the mean shear. As the mean pressure gradient is zero the linear contribution of $\rho'/\bar{\rho}$ can be neglected. It is then likely that the observed spreading rate of such flows can be related to mechanisms neglected in the present analysis, for example the modifications to pressure transport or return-to-isotropy brought about by density gradients or density fluctuations.

2.4. *Models used in the present work*

The equations used to determine the Reynolds stress tensor are the following:

$$\frac{\mathrm{D}}{\mathrm{D}t}T_{ij} = -T_{ik}(D_{jk}+R_{jk}) - T_{jk}(D_{ik}+R_{ik}) + \alpha(i)\frac{(\gamma-1)M^2}{\bar{\rho}\tilde{u}}T_{1i}\frac{\partial\bar{p}}{\partial x_j} + \alpha(\mathrm{j})\frac{(\gamma-1)M^2}{\bar{\rho}\tilde{u}}T_{1j}\frac{\partial\bar{p}}{\partial x_i} + \pi_{ij}, \quad (13)$$

with

$$\alpha(i) = R_{T1} \quad \text{if } i = 1,$$
$$= \frac{R_{T2}}{R_{12}} \quad i = 2,$$
$$= 0 \quad i = 3,$$

and

$$\pi_{ij} = (\pi_{ij})_u + (\pi_{ij})_p.$$

$(\pi_{ij})_u$ and $(\pi_{ij})_p$ are the contribution to π_{ij} of the mean velocity gradient and of the mean pressure gradient, respectively.

Three different models will be used for $(\pi_{ij})_u$:

Launder, Reece & Rodi (1975) (LRR)

$$(\pi_{ij})_u = T_{kk}[\tfrac{2}{5}D_{ij} + 0.87(a_{qj}D_{iq} + a_{qi}D_{jq} - \tfrac{2}{3}a_{ql}D_{lq}\delta_{ij}) + 0.656(a_{qi}R_{jq} + a_{qj}R_{iq})],$$

$$a_{qj} = \frac{T_{qj}}{T_{ii}} - \tfrac{1}{3}\delta_{qj}.$$

Lumley (1975) (L)

$$(\pi_{ij})_u = T_{kk}[\tfrac{2}{5}D_{ij} + \tfrac{12}{7}(a_{qi}D_{jq} + a_{qj}D_{iq} - \tfrac{2}{3}a_{ql}D_{lq}\delta_{ij})].$$

Naot, Shavit & Wolfsthein (1970) (NSW)

$$(\pi_{ij})_u = T_{kk}[\tfrac{2}{5}D_{ij} + \tfrac{3}{5}(a_{qi}D_{jq} + a_{qj}D_{iq} - \tfrac{2}{3}a_{ql}\delta_{ij}) + \tfrac{3}{5}(a_{qi}R_{jq} + a_{qj}R_{iq})].$$

To represent $(\pi_{ij})_p$, only one model was retained (Lumley 1975):

$$(\pi_{ij})_p = -0.3\left(\frac{\overline{T'u_i'}}{\bar{\rho}\tilde{T}}\frac{\partial p}{\partial x_j} + \frac{\overline{T'u_j'}}{\bar{\rho}\tilde{T}}\frac{\partial p}{\partial x_i} - \frac{2}{3}\frac{\overline{T'u_k'}}{\bar{\rho}\tilde{T}}\frac{\partial p}{\partial x_k}\delta_{ij}\right).$$

A brief comparison can now be made between the hypothesis in the present analysis and those used by Goldstein (1978) to calculate the rapid distortion in a centred expansion.

Goldstein chooses isotropic initial conditions for the fluctuations. This choice, although of great importance for the actual evolution of turbulent kinetic energy in the distortion, does not basically change the physics of the problem; the condition of homogeneity is not required, the turbulent velocity can have a non-zero divergence and the low-wavenumber range is calculated without approximation. Since pressure fluctuations are calculated no particular assumption is needed. On the other hand, the mean entropy must be constant and the mean flow irrotational.

In the present analysis, the velocity field is required to remain solenoidal and the temperature fluctuations are assumed to be practically isobaric everywhere in the flow. Pressure fluctuations are modelled, and since the 'pressure transport' is neglected, the turbulent field is supposed to be weakly inhomogeneous. However, the models can be applied to flows with entropy gradients and mean vorticity. Features common to the two analyses are the neglect of viscous and nonlinear effects, i.e. for second-order closure, the neglect of dissipation, turbulent diffusion and return-to-isotropy terms. In §5, we will compare predictions of the Reynolds-stress transport equations, using the present simplifications and the above models for π_{ij}, with the measurements described in §§3 and 4.

3. Experimental arrangement and measurement techniques

Measurements were performed in the IMST continuous supersonic wind tunnel. The cross-section of the nozzle is 10×15 cm^2. A 1 cm thick fully turbulent boundary layer developed on the floor of a half-nozzle, and at the station upstream of the expansion the Reynolds number based on momentum thickness was 5000. The nominal free-stream Mach number was 1.76 and the stagnation pressure was 40530 N/m^2. Fifteen minutes after starting the tunnel the recovery factor was 0.91 and therefore the wall conditions were practically adiabatic. Transition was triggered by a roughness strip placed upstream of the throat. Mean velocity profiles and turbulence spectra showed that, at a stagnation pressure of 26000 N/m^2, transition was achieved well upstream of the zone where the present measurements were performed.

A 12° deflection of the wall around a sharp edge produced an expansion fan by a turning without separation. The experimental configuration and the coordinate system is shown in figure 1.

Total pressure, static pressure and total temperature profiles were measured. The total pressure measurements were performed with flattened Pitot probes. We used

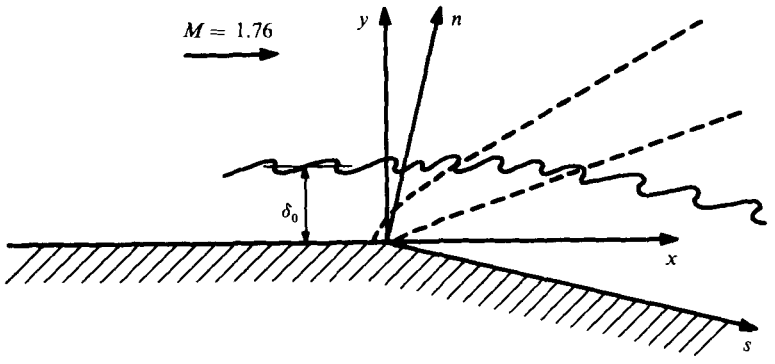

FIGURE 1. Sketch of the flow.

Voisinet & Lee's calibration (1972) to check that no low-Reynolds-number correction was required. Spatial integration errors were estimated from Allen (1972); it was found that the maximum error was comparable to the uncertainties in the probe location, and no correction was therefore applied.

Upstream and downstream of the expansion, the wall static pressure was measured using pressure taps. In the free stream, the static pressure was deduced from Pitot probe measurements. Out of the viscous sublayer, the expansion zone can be considered as a vortical perfect fluid flow, if the pressure gradient is much larger than the friction force (see for example Délery & Masure 1969). The flow can then be computed from the Euler equations by the method of characteristics. In our case, it was estimated, from the analysis proposed by Narasimha & Viswanath (1975), that the pressure gradient is about a hundred times as large as the friction force. This method was then used in our case to compute the mean static pressure and other mean quantities within the expansion. The results are probably more accurate than measurements performed with a static pressure probe, for this type of probe can perturb the expansion fan, and is very sensitive to yaw.

The total temperature was measured in the supersonic part of the flow ($M > 1.3$), with hot-wire probes using the method of Laufer & McClellan (1956). The wire diameter was 5 μm and the aspect ratio was 300. The wall temperature was checked by BTE–CTE thermocouples inserted in the wall, and good agreement with the extrapolated hot-wire results was found.

Turbulence measurements were made with hot-wire probes. The filament was platinum-plated tungsten with a diameter of 2.5 μm and an aspect ratio of 320. The wires were welded to steel prongs with sufficient slack to avoid strain gauging: wires with spurious strain-gauging signals greater than 3 % of the total signal r.m.s. value were discarded.

The anemometer was of the constant-current type, manufactured by Shapiro and Edwards, South Pasadena, CA. The uncompensated amplifiers were modified to have a 320 kHz bandwidth and to improve the signal-to-noise ratio. According to Kistler (1959), more than 90 % of the signal variance in zero-pressure gradient boundary layers is captured if the amplifier bandwidth is greater than 4 U_∞/δ. In our flow U_∞/δ is typically 50 kHz, so that Kistler's criterion is well fulfilled. The hot wire was compensated for thermal lag effects and the time constant was measured *in situ* for each point using a square-wave-current injection method.

The temperature and velocity fluctuations were separated using Kovasznay's

fluctuation diagram technique and the sensitivity coefficients were determined as in Gaviglio (1971, 1978). The diagrams were obtained by operating the wire at 14 different overheat ratios a'_w in the range $0.02 \leqslant a'_w \leqslant 0.5$ and hyperbolas were fitted through the points by a least-squares method. A preliminary study determined that the value of the turbulent intensity of velocity and/or temperature could be affected if less than 12 points was used.

The measurements were corrected for noise and the imperfections of the compensating circuit according to Gaviglio & Dussauge (1977) and Gaviglio (1978). In the previous references, it is stressed that the imperfections result in a bandwidth limitation which depends on the time-constant value; a correction method is proposed, based on the knowledge of the time constant and of the initial curvature of the erroneous signal autocorrelation; this method proved to be very effective, even in severe situations. In the present experiment, the corrections applied to the r.m.s. signal value typically ranged between 5% for low overheat ratios and 15% for $a'_w = 0.5$. Autocorrelations were measured with delay lines (Adyu Electronics) and a home-made analogue correlator; the bandwidth of each instrument was at least 350 kHz.

4. Experimental results

4.1. *Upstream of the expansion zone*

The properties of the incoming boundary layer are summarized in table 1, where δ_0, δ^*, θ are respectively the boundary-layer thickness ($\tilde{u}_1/u_e = 0.999$), the displacement thickness, and the momentum thickness.

The mean velocity profiles of the incoming boundary layer were plotted using the Van Driest transformation

$$V = \int_0^{\tilde{u}_1} \left(\frac{\bar{\rho}}{\bar{\rho}_w}\right)^{\frac{1}{2}} \mathrm{d}u' \tag{14}$$

(see for example, Fernholz & Finley, 1980), where V was determined from $\bar{\rho}$ and $\tilde{u}_1$ measurements. The friction coefficient C_f and the friction velocity u_τ were deduced from the slope of the logarithmic profiles by assuming that the von Kármán's constant is 0.41. The result is given on figure 2, which presents $V^+ = V/u_\tau$ versus $y^+ = y\,u_\tau/\nu_w$; ν_w is the wall kinematic viscosity. These data agree well with the relation

$$V^+ = \frac{1}{\chi} \ln y^+ + B, \tag{15}$$

for $30 < y^+ < 200$ and $B = 5$. However, a more precise fit can be achieved by taking $B = 5.7$. The uncertainty could be due to the determination of V from experimental values of $\bar{\rho}$ and $\tilde{u}_1$. The computation of the integral in (14) is difficult in the range $0 < \tilde{u}_1/u_e < 0.4$ because of the lack of resolution very near the wall. The same interpolation was used near the wall for all the profiles, and therefore the same departure from $B = 5$ can be systematically introduced. The skin friction coefficient used is given in figure 3 and the experimental values compare favourably with Michel's correlation (1960).

Figure 4 shows $\widetilde{u_1'^2}$ measurements in the initial boundary layer using Morkovin's representation. The scatter of the data is rather large. This can be due to the uncertainties on $\widetilde{u_1'^2}$, u_τ or δ. However, the present measurements are consistent with the other data in the zone where the Mach number is greater than 1.3.

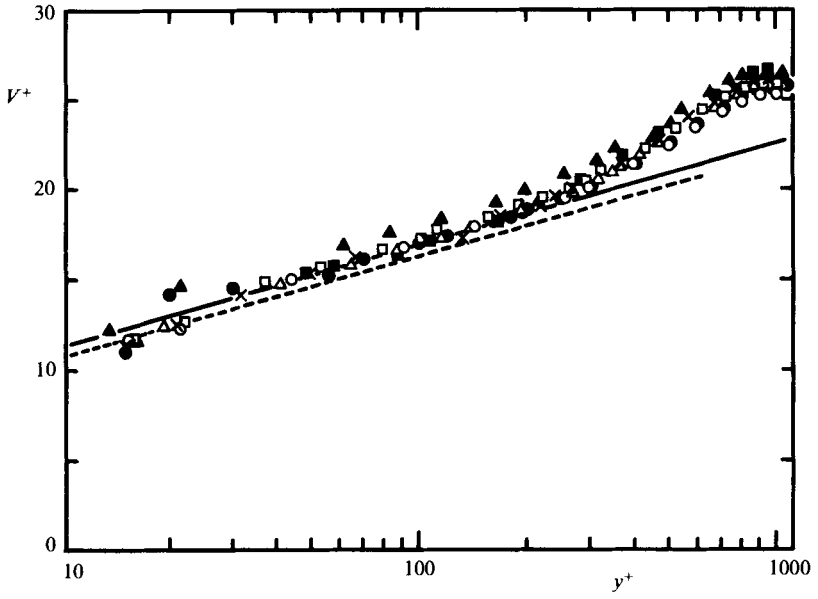

FIGURE 2. Mean velocity profiles in the initial boundary layer (Van Driest's transformation). ▲, x, −62.5 mm; ○, −52.5 mm; □, −42.5 mm; ×, −32.5 mm; △, −22.5 mm; ●, −10 mm; ■, −5 mm; ---, $V^+ = \ln y^+/\chi + 5$; ——, $V^+ = \ln y^+/\chi + 5.7$.

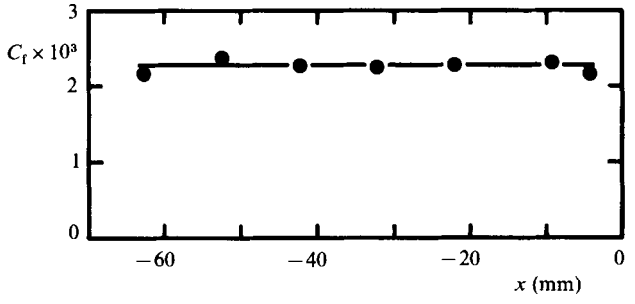

FIGURE 3. Friction coefficient in the initial boundary layer.

In addition, the SRA relation between temperature and velocity fluctuations (equation (1)) appears to be substantiated in the main part of the layer (figure 16) and the velocity temperature correlation coefficient R_{T_1} has a nearly constant value of 0.8 (see figure 15).

4.2. *Expansion zone*

As indicated in §3, the mean field can be determined outside the viscous sublayer by the method of characteristics, if it is assumed that the entropy and total enthalpy are constant along a mean streamline. The measurements showed that the total temperature was virtually constant in the expansion and therefore the method of characteristics was used to find the mean field. The inner boundary condition was set by the streamline which was initially sonic, and it was assumed that this streamline suffered a 12° deflection; its shape was approximated to be consistent with the Pitot measurements. The results of the calculation are in good agreement with

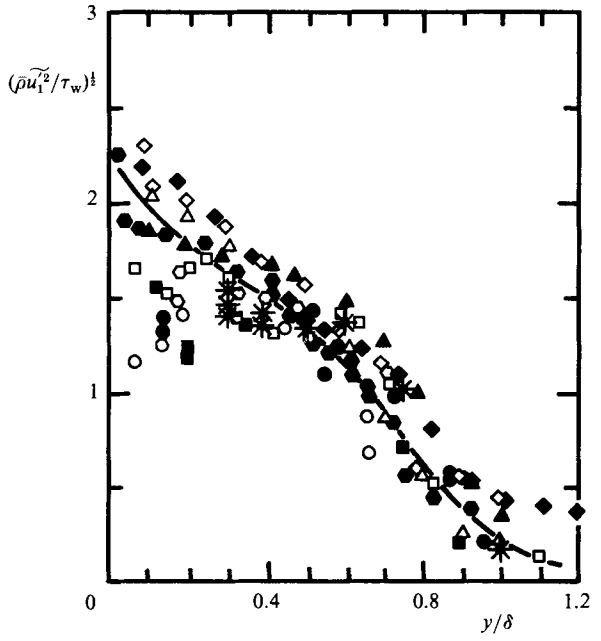

FIGURE 4. Velocity fluctuation in the upstream boundary layer. *, present data; ○, $M = 1.72$; ●, $M = 3.56$; ○, $M = 4.67$ (Kistler 1972); $M = 2.9$: △, hot-wire; ◇, laser (Johnson & Rose 1975); (▲, Smits *et al.* (1983); ■, Elena *et al.* (1977); □, Debieve (1983); ⬢, Elena & Gaviglio (1983); ◆, Yanta & Crapo (1976).

x (mm)	δ_0 (mm)	θ (mm)	M_e	R_θ	C_f
−5	10	0.88	1.76	5000	2.25×10^{-3}

TABLE 1. Properties of the incoming boundary layer

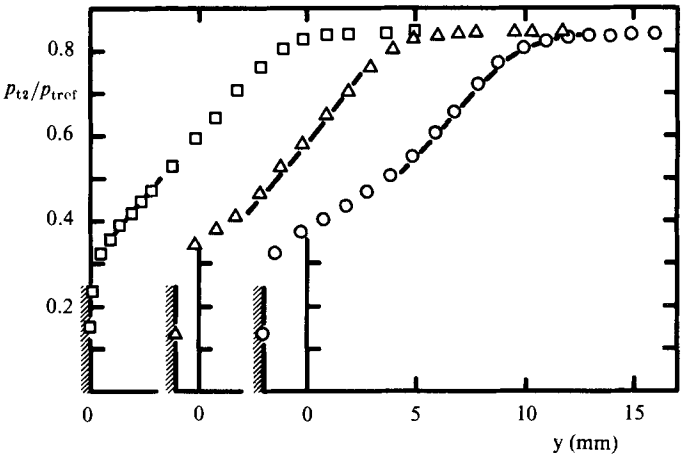

FIGURE 5. Pitot pressure profiles, ——, calculation; measurements: □, $x = 0$; △, $x = 5$ mm; ○, $x = 10$ mm.

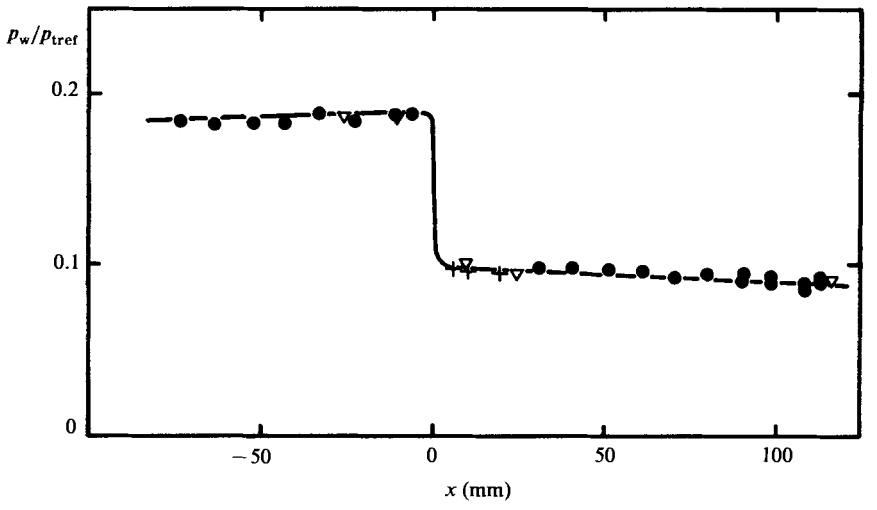

FIGURE 6. Mean wall pressure. ●, static pressure probes; ▽, wall pressure taps; +, calculated (method of characteristics).

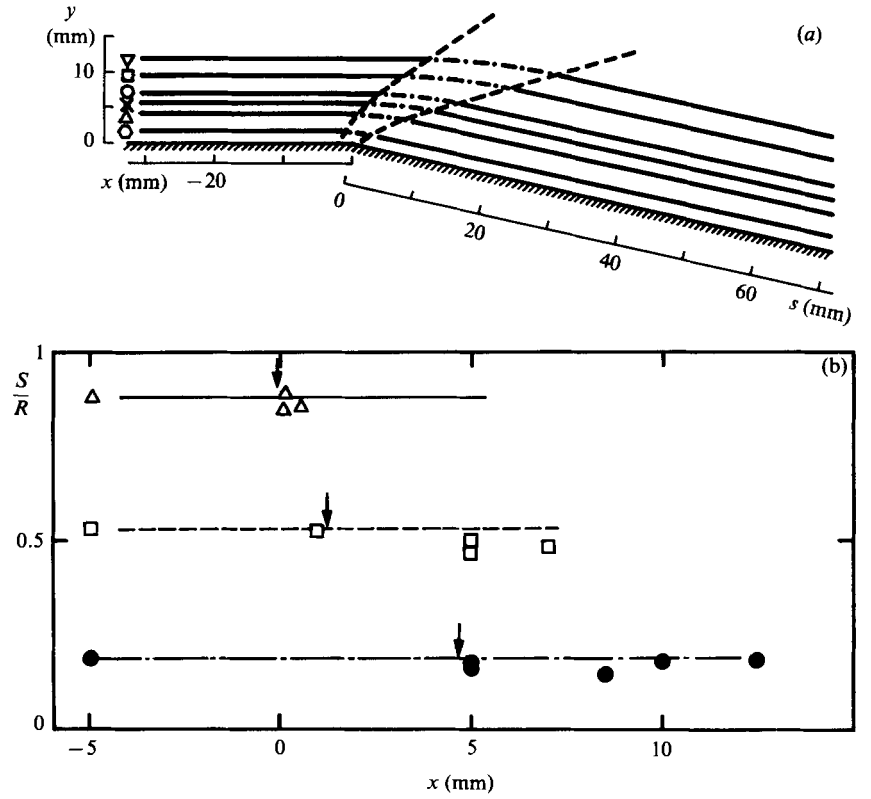

FIGURE 7. (*a*) Mean streamlines. —·—, calculated; measured: ▽, $Q^* = 0.4$; □, $Q^* = 0.3$; ○, $Q^* = 0.2$; ×, $Q^* = 0.15$; △, $Q^* = 0.1$; ⬡, $Q^* = 0.03$. (*b*) Mean entropy distribution along streamlines; the constant values used in the calculation are represented by lines. Arrows indicate the beginning of the expansion. Measurements: △, $Q^* = 0.05$, $(y/\delta)_0 = 0.25$; □, $Q^* = 0.1$ $(y/\delta)_0 = 0.43$; ●, $Q^* = 0.2$ $(y/\delta)_0 = 0.72$.

Pitot measurements, as shown in figure 5 where p_{t2} is the Pitot pressure, i.e. the stagnation pressure downstream of a plane shock wave, and p_{tref} is the total pressure in the outer flow. The computed wall-pressure values are compared with the measurements in figure 6.

Figure 7 gives the mean streamlines defined as the isocontours of the mass flux

$$Q^* = \int_0^y \frac{\bar{\rho}\tilde{u}_1 \,\mathrm{d}y}{\rho_{\text{tref}} a_{\text{tref}} \delta_0},$$

where a_{tref} is the sound speed determined from stagnation quantities in the outer flow. Upstream and downstream of the interaction $\bar{\rho}\tilde{u}_1$ was obtained experimentally, whereas in the expansion fan the mass flux was deduced from the computation and there appears to be a good agreement between the two determinations. The favourable comparison between measurements and computation is not very surprising. The calculation assumed that the pressure gradient is much larger than the friction force, the total enthalpy and entropy being constant along a mean streamline. As reported in §3, the first condition is fulfilled in the expansion fan. Measurements showed that the total temperature remains nearly constant: as we are outside the viscous sublayer, only the turbulent diffusion can affect the total enthalpy. Since we consider evolutions over a small distance, the integral of diffusion terms along this distance is itself small. A quantitative justification of this assessment is proposed in Appendix C. It leads to the conclusion that the variation of total temperature ΔT_t after a length L_d can be approximated by $\Delta T_t \; (L_d/\Lambda) \; (-\widetilde{u_1' u_2'}/C_p)$; Λ is a typical lengthscale for momentum diffusion, for example the initial boundary thickness. In our case, this corresponds to a variation ΔT_t of about 1 °K. The last point is to show that the mean entropy does not vary much in a rapid distortion without shock wave. Sources of entropy are turbulent diffusion, viscous dissipation or heat conduction. In Appendix C the details of an order-of-magnitude analysis are given. In particular it is recalled that in supersonic boundary layers these three contributions are comparable. It is shown that a typical value of the entropy sources is given by the rate of dissipation, which is practically constant in a rapid expansion. It follows that the variation of entropy Δs in a rapid distortion of spatial extent L_d is of the order of $\gamma R(Ld/\Lambda_0)(q_0'/U)/m_0^2$. R is the perfect gas constant, m_0 the Mach number of velocity fluctuations before the expansion, $m_0 = q_0'/(\gamma R T_0)^{\frac{1}{2}}$. If the mean entropy S_0 is nearly constant, then $\Delta s/S_0 \ll 1$. If the total enthalpy is constant, S_0 is defined in the upstream boundary layer by

$$S_0 = R \ln (p_t/p_{\text{tref}})_0 = R \ln (1 + \tfrac{1}{2}(\gamma - 1) M_0^2) \frac{\gamma}{(\gamma - 1)}.$$

The condition to be fulfilled is then:

$$(\gamma - 1) \frac{Ld}{\Lambda_0} \frac{q_0'}{U} \frac{m_0^2}{\ln (1 + \frac{1}{2}(\gamma - 1) M_0^2)} \ll 1.$$

As in a rapid distortion $(L_d/\Lambda_0)(q_0'/U_0) \ll 1$, a sufficient condition for constant entropy is:

$$\frac{m_0^2}{\ln (1 + \frac{1}{2}(\gamma - 1) M_0^2)} \ll 1.$$

Entropy is then expected to change if m_0 is large and M_0 small. In our particular calculation, the more severe situation is found on the sonic line where $m_0 < 0.1$; with

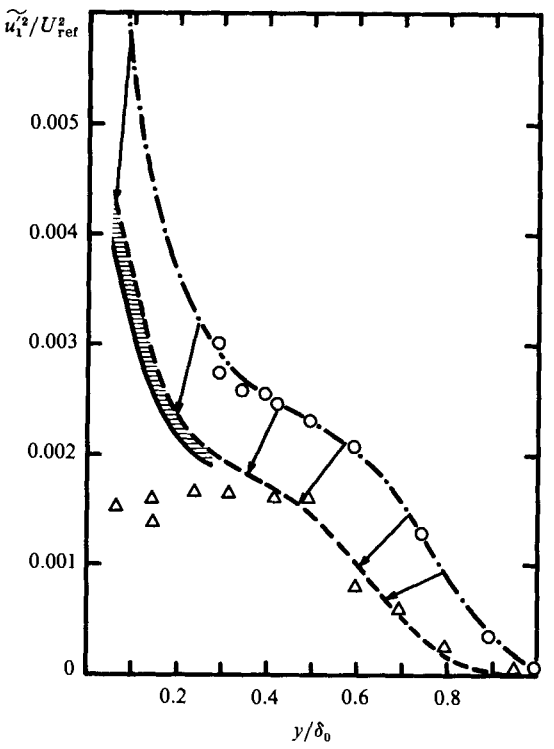

FIGURE 8. Velocity fluctuations in the distortion. ○, upstream profile; △, along the last Mach wave; – – –, dilatation effect; shaded zone, dissipation effect. Arrows indicate streamline correspondence.

this value the inequality is satisfied. Examples are given in figure 7 (*b*), which presents the entropy along particular streamlines. Experimental values are obtained by interpolation and the constant values used in the calculation are represented by lines. It appears that the entropy can be considered as constant.

Turbulence measurements were performed normal to the floor upstream of the expansion, along the last Mach wave, and along two streamlines ($Q^* = 0.063$ and $Q^* = 0.21$) which are initially located at $y/\delta_0 = 0.3$ and 0.8 respectively. A decrease of $\widetilde{u'^2}$ is observed through the expansion (figures 8 and 9). A similar variation was deduced by Sternberg (1954) from calculations based on Ribner & Tucker's theory (1952); it was also found experimentally by Morkovin (1955) in an expanded boundary layer with a flow geometry different from the present one, and by Gaviglio *et al.* (1977) in a near wake flow.

Velocity spectra were measured upstream and downstream of the expansion among the two streamlines. The results are given in figure 10 and were partly reported by Bestion, Debiève & Dussauge (1983). These measurements are rather scattered. However, it appears that along the outer streamline ($Q^* = 0.21$), no major change in the shape of the spectral density is found for frequencies higher than 10 kHz. Along the internal streamline ($Q^* = 0.063$), the spectral density changes slightly for $n > 10$ kHz.

4.3. *Downstream of the expansion zone*

The expansion strongly perturbs the boundary layer; for example, the ratio $|\Delta p|/\tau_{w_0}$, where Δp is the pressure drop and τ_{w_0} the initial wall friction, is about 100. According

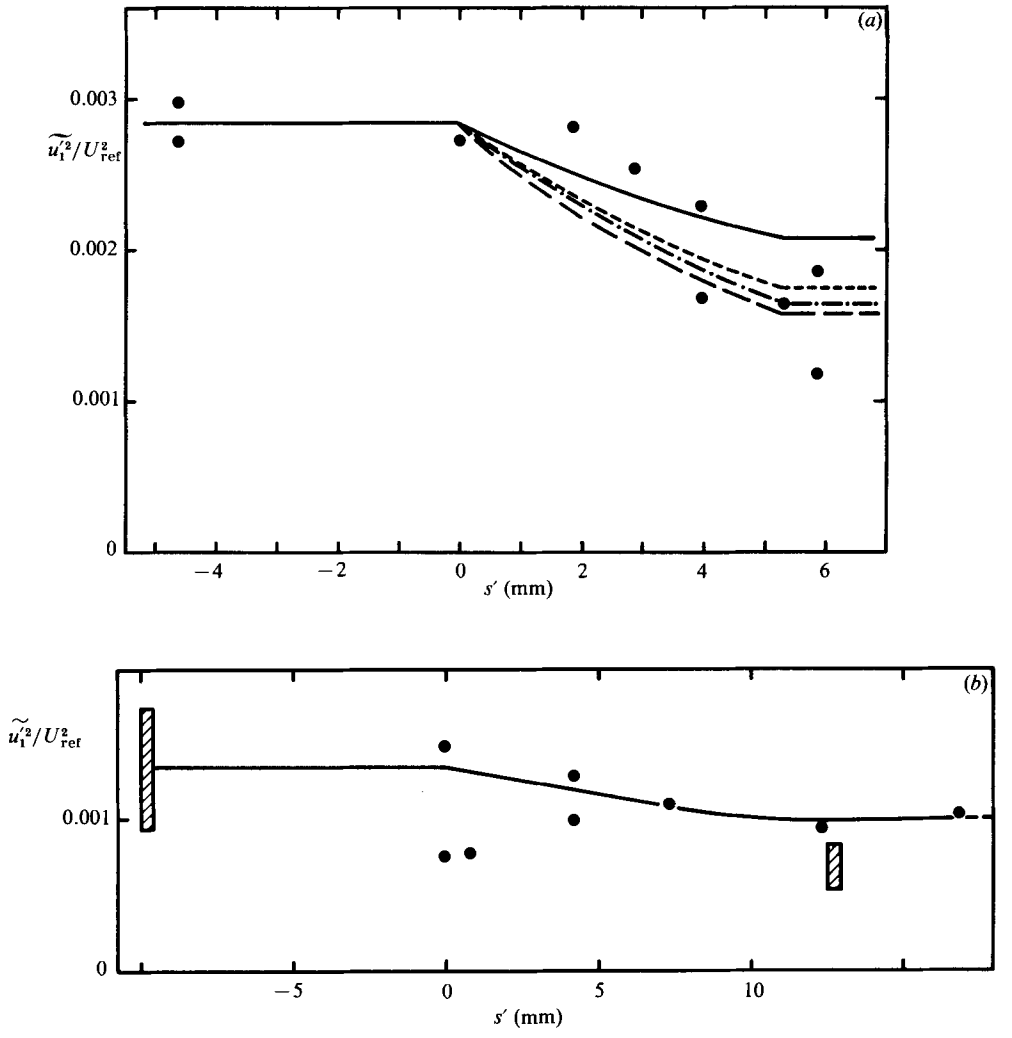

FIGURE 9. $\widetilde{u'^2}$ variation in the expansion. (*a*) $Q^* = 0.063$; ●, measurements; ——, effect of dilatation; – – –, model L; —·—, LRR; – – –, NSW. (*b*) $Q^* = 0.21$; shaded zone, upstream and downstream levels deduced from figure 8.

to Narasimha and Viswanath (1975), the boundary layer should exhibit features of 'relaminarization'. In addition, as can be seen from figure 6, there is a slight longitudinal pressure gradient and the value of the Clauser parameter $\delta^*(\partial\bar{p}/\partial s)/\tau_w$ is about -0.25. However, such a low pressure gradient should not significantly affect the return of the boundary layer to equilibrium.

The Van Driest transformed velocity profiles are shown on figure 11. No significant evolution is found in the external part of the profiles. In the initial stage (31.3 mm $\leqslant s \leqslant$ 90 mm) a rather thick sublayer is found close to the wall with a larger velocity gradient, and the semi-logarithmic plot shows an inflection point, rather than a linear evolution, away from the sublayer. For $s > 90$ mm, a linear part is found and it seems that a new wall region is formed.

The skin friction was determined from the mean measurements by four different

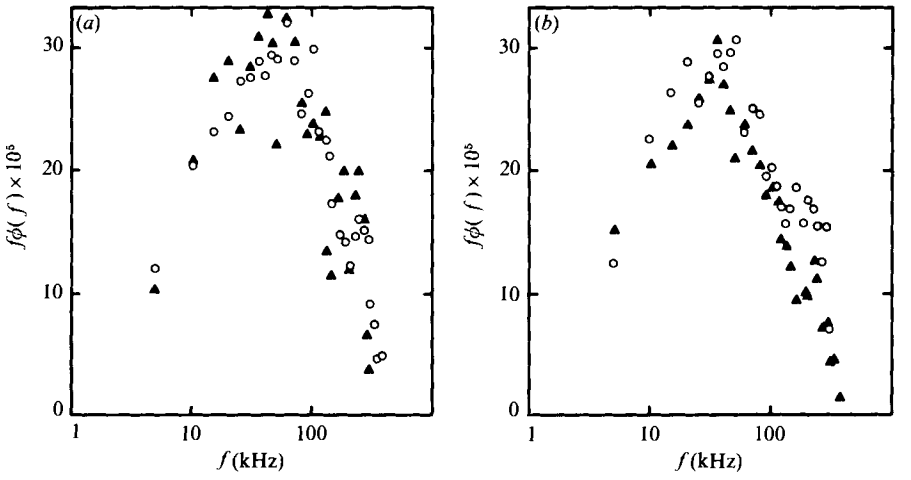

FIGURE 10. Velocity spectra. (*a*) $Q^* = 0.21$ ($y/\delta_0 = 0.8$); ▲, upstream; ○, downstream. (*b*) $Q^* = 0.063$ ($y/\delta_0 = 0.3$); ▲, upstream; ○, downstream.

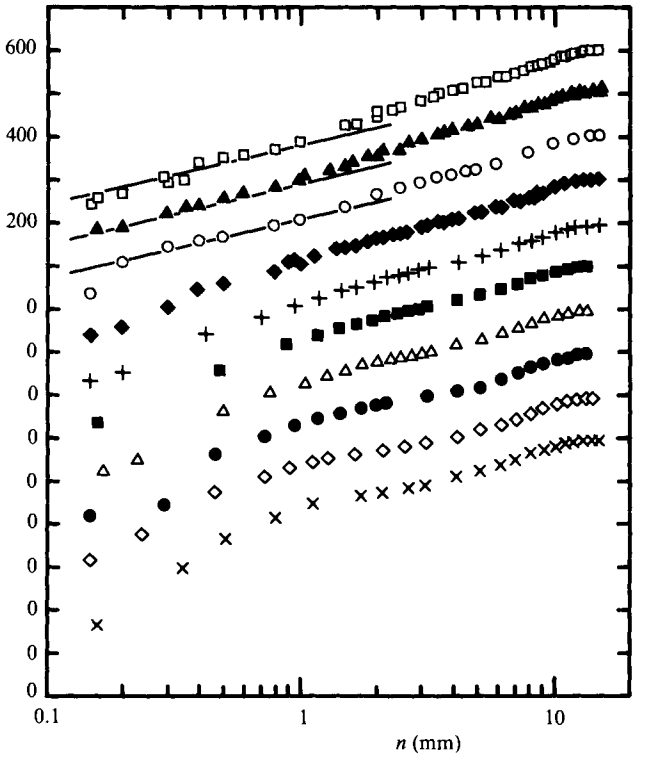

FIGURE 11. Mean velocity profiles downstream of the expansion (Van Driest's transformation). $s = 31.3$ mm; ◇, $s = 40.5$ mm; ●, $s = 50.9$ mm; △, $s = 61.5$ mm; ■, $s = 70.5$ mm; $s = 79$ mm; ◆, $s = 89.5$ mm; ○, $s = 98$ mm; ▲, $s = 108$ mm; □, $s = 113$ mm.

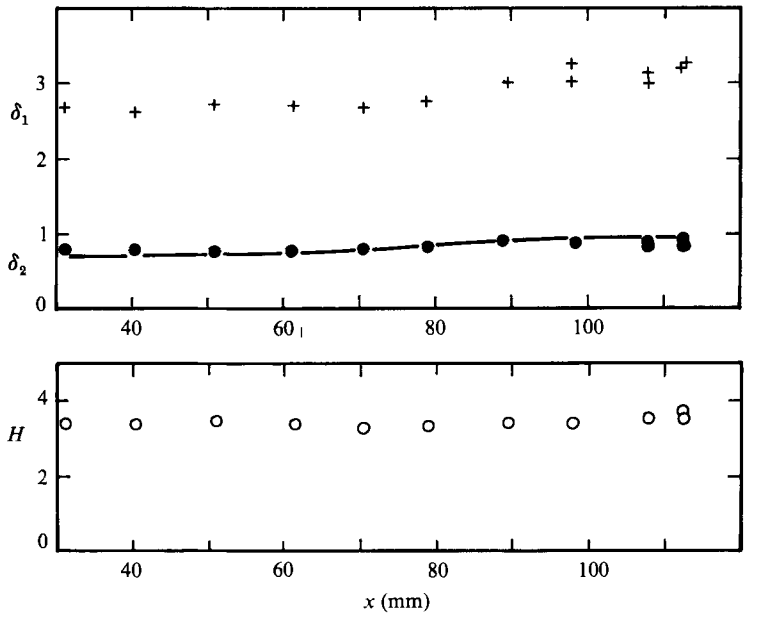

FIGURE 12. Integral parameters downstream of the expansion. ——, C_f determined from Chew (1978). +, δ_1 mm; ●, δ_2 mm.

methods. Two methods were based on a momentum balance and the first method uses the momentum equation expressed in terms of $\bar{p}$ and p_t (see Bradshaw 1974).

$$\frac{\partial \tau}{\partial n} = -\frac{\bar{p}}{p_t}\frac{\partial p_t}{\partial s}. \tag{16}$$

The second method uses von Kármán's integral equation; the displacement thickness δ^*, the momentum thickness θ and the shape parameter H given in figure 12.

The third method uses Chew's correlation (1978)

$$C_f = 0.246\left(\frac{\rho_w}{\rho_e}\right)^{0.8} 10^{-0.678H^*} R_{\delta_2^*}^{-0.268}, \tag{17}$$

with

$$H^* = \frac{\delta_1^*}{\delta_2^*},$$

$$\delta_1^* = \int_0^\delta \left(\frac{1-V}{V_e}\right) \mathrm{d}n,$$

$$\delta_2^* = \int_0^\delta \frac{V}{V_e}\left(\frac{1-V}{V_e}\right) \mathrm{d}n,$$

and V is defined according to (14). Equation (17) is in good agreement with Preston tube measurements in an expanded supersonic boundary layer (Chew & Squire 1979).

Finally, C_f was evaluated from the mean velocity profile slope in semi-log representation, and it depends on the validity of the law of the wall. If the results are consistent with those given by the other methods, it may show that the law of the wall is re-established. As suggested by Bradshaw (private communication 1981),

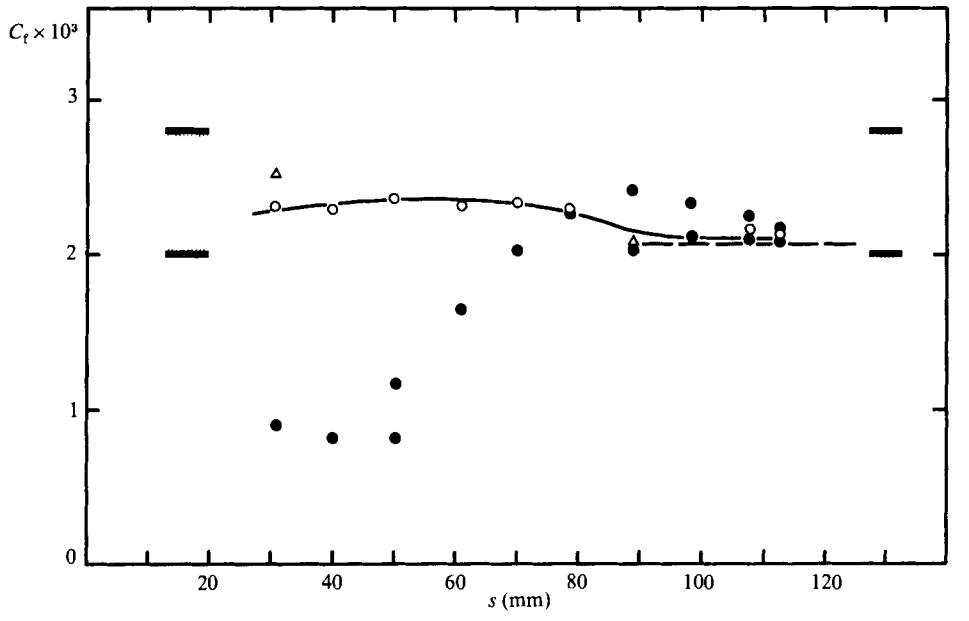

FIGURE 13. Friction coefficient downstream of the expansion. Shaded area, range of the results given by the von Kármán equation; ○, formula (17); △, momentum balance; ●, slope of the logarithmic profiles; ----, equilibrium value.

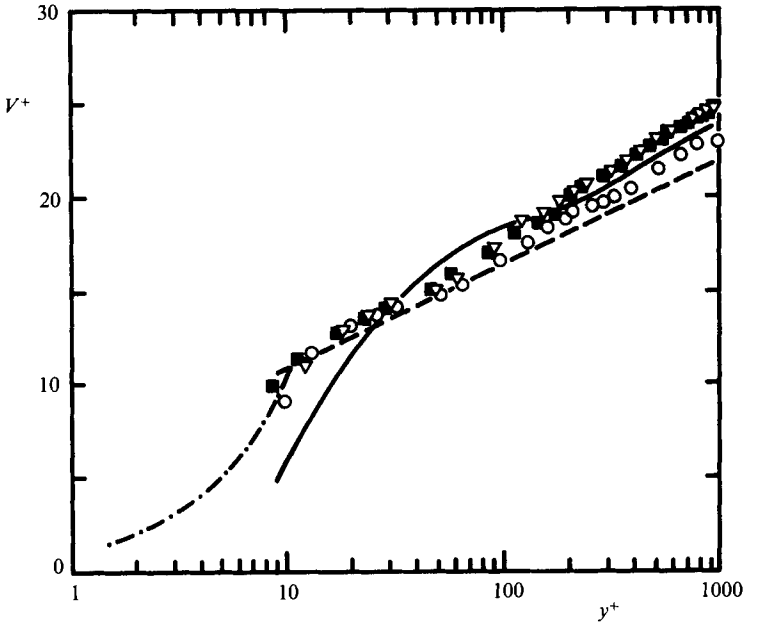

FIGURE 14. The law of the wall in the relaxing boundary layer. ——, $s = 31.3$ mm; ○, $s = 98$ mm; □, $s = 108$ mm; ▽, $s = 113$ mm; ----, $V^+ = (1/\chi) \ln n^+ + 5.0$; —·—, $V^+ = n^+$.

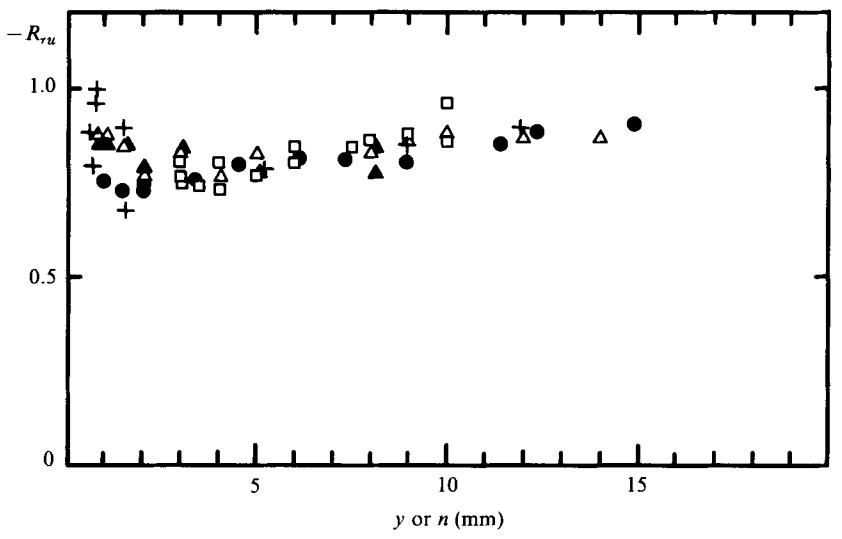

FIGURE 15. Velocity temperature correlation coefficient. □, $x = -5$; ●, downstream characteristic; +, $s = 31.3$ mm; ▲, $s = 89.5$ mm; △, $s = 98$ mm.

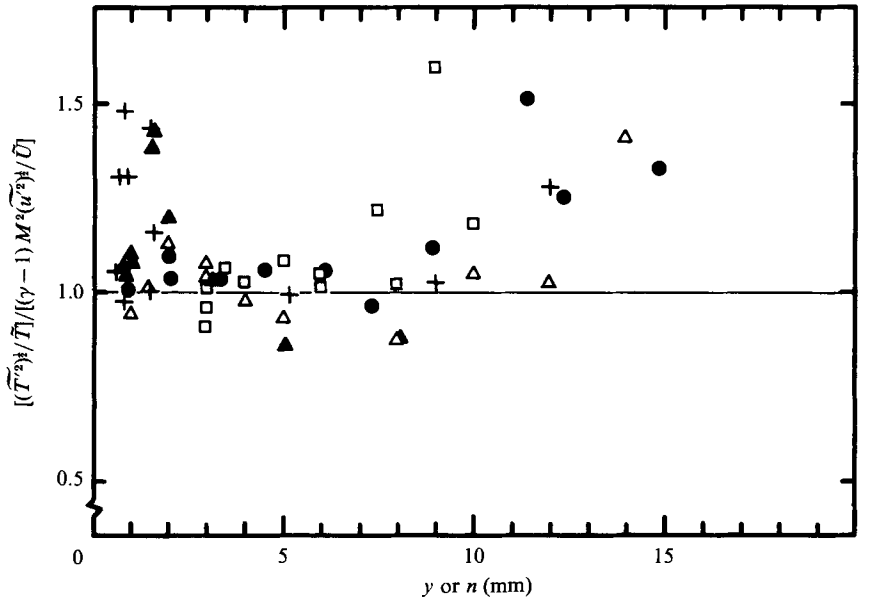

FIGURE 16. Strong Reynolds analogy. Symbols as for figure 15.

C_f is most easily obtained by adjusting the value of V^+ for a given n^+, rather than by determining the slope of the profile. However, the value of B is the subject of some uncertainty. As discussed previously, it seems that a value of 5.7 describes the present results better than a value of 5.0. Finally, C_f was determined with $B = 5$ for all the profiles; in the last four sections, a determination was also made with $B = 5.7$.

The results are given in figure 13. The use of von Kármán's equation depended critically on the curve-fitting of the experimental data, and it gave very scattered

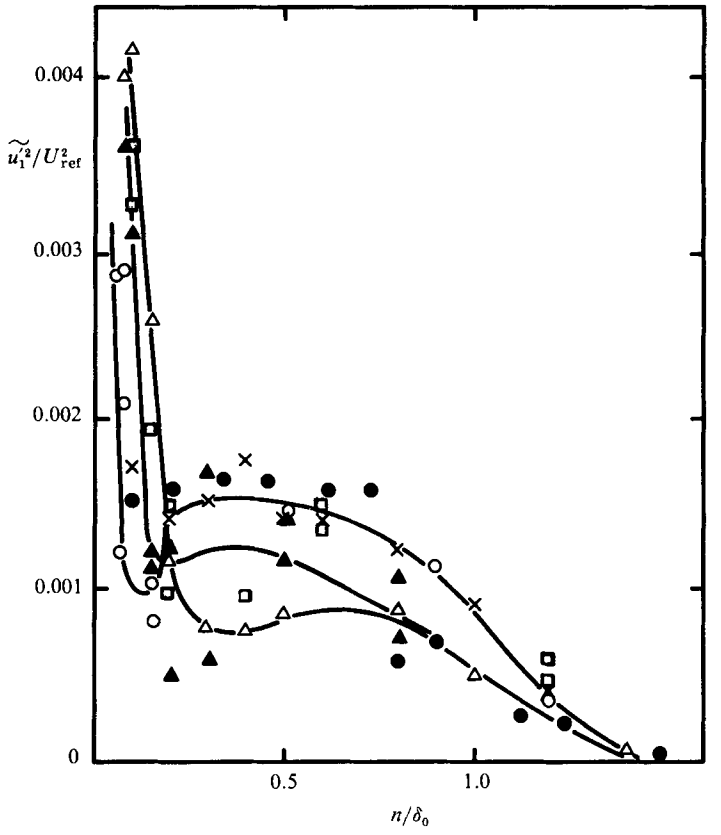

FIGURE 17. Velocity fluctuations in the relaminarized boundary layer. ●, last expansion characteristic; ○, ×, $s = 31.3$ mm; □, $s = 61.5$ mm; ▲, $s = 89.5$ mm; △, $s = 98$ mm.

values. The momentum balance (equation (16)) gave results consistent with Chew's formula (Chew 1978), despite the rather short length over which the longitudinal derivatives could be evaluated.

The C_f values given by (17) were checked for consistency with the measured momentum thickness by integration von Kármán's equation to determine θ, using C_f from (17) as an input. The result, given in figure 12, is satisfactory, in spite of the discrepancy found at $s = 31.3$. This result, and the rather high values of C_f given by the momentum balance (equation (16)) at $s = 31.3$, could suggest flow divergence immediately downstream of the expansion. Surface flow visualizations, however, showed no particular spanwise streamline divergence. Moreover, an estimate of the measurement errors showed that the scatter of the data is comparable to the uncertainties on θ. For $s \geqslant 90$ mm, the law of the wall values is consistent with the other determinations, and they also agree well with the C_f for an equilibrium boundary layer at the same Mach number and momentum-thickness Reynolds number. Some typical V^+ profiles are shown on figure 14. For the station at $s = 31.3$ mm, u_τ was calculated from (17). It can be seen that the shape of the profiles, close to the wall, changes considerably between $s = 31.3$ mm and $s = 98$ mm. Downstream, similarity is found for $10 < n^+ < 80$.

As mentioned earlier, the turbulence measurements show that the correlation coefficient R_{T1} remains virtually constant in the whole field (figure 15); besides, the SRA relation (1) holds reasonably well at all stations, $y/\delta < 0.8$ (figure 16). Some

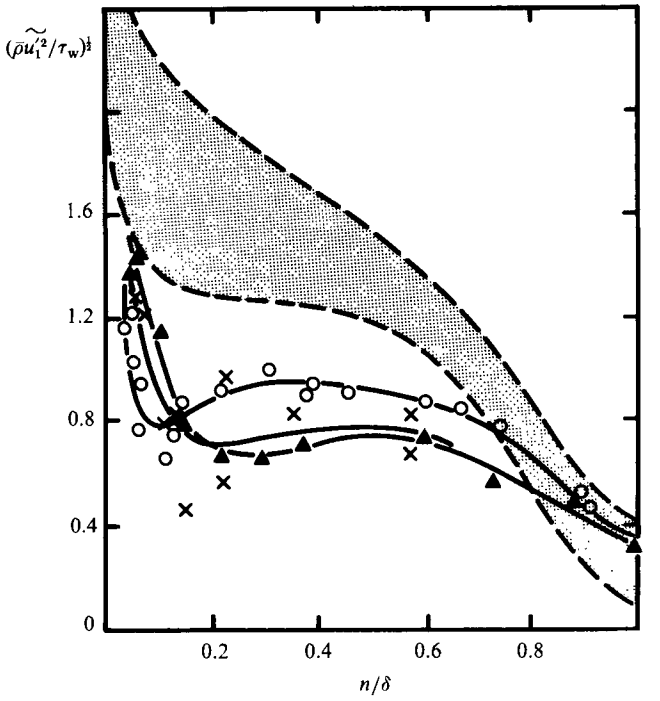

FIGURE 18. Dimensionless representation of velocity fluctuation profiles. Shaded zone, equilibrium measurements; ○, $s = 31.3$ mm; ×, $s = 89.5$ mm; ▲, $s = 98$ mm.

discrepancies are observed in the outer part of the boundary layer, but here the intermittent nature of the flow probably reduces the accuracy of hot-wire measurements.

The longitudinal velocity fluctuations $\widetilde{u_1'^2}$ (figure 17) show that for $n/\delta_0 > 0.25$, $\widetilde{u_1'^2}$ decreases slightly, whereas near the wall the $\widetilde{u_1'^2}$ level is initially very low. The same results are plotted in figure 18 in Morkovin's representation. Immediately downstream of the expansion, the results lie well below the range of the flat plate data; this was expected for a relaminarized boundary layer. At the last two stations ($s = 89.5$ mm, 98 mm) $\widetilde{u_1'^2}$ for $n/\delta < 0.1$ begins to recover to an equilibrium level. Thus, the boundary layer appears to recover to a self-similar state, and the mean and turbulent measurements are consistent with the description of relaminarized boundary layers (Narasimha & Sreenivasan 1979) and some properties of perturbed boundary layers (Smith & Wood 1985): in the outer part of the flow the evolutions, which are probably governed by diffusive and dissipative processes, are slow; near the wall, where large mean gradients (and production terms) exist, an internal layer is created, growing and gradually changing the properties of the whole layer.

5. Discussion

First, we shall check whether the rapid distortion requirements are fulfilled. For this purpose, we need a definition of the 'integral' scale Λ. In subsonic flat-plate boundary layers, a typical value is $0.4\,\delta$, in supersonic boundary layers the measurements of Bestion *et al.* (1983) show that $0.25\,\delta$ is probably a better estimate. This result seems inconsistent with the proposed analysis in which turbulent scales are proposed to be unaffected by compressibility. The measurements were performed by

extrapolating spectra of the hot-wire signal to zero frequencies and then using the fluctuation diagram technique. This procedure is of limited accuracy partly because of the extrapolation and partly because the heat loss through the prongs of a finite-length hot wire can attenuate the signal at very low frequencies. Moreover (6) and (7) show that a density gradient can change the pressure in a limited range located at very low frequencies (in the present case $n > 3$ kHz) and that this low frequency range and the rest of the energy range can have different behaviours. Since the contribution of the very low frequencies to the velocity variance is small, the latter remains practically unchanged. It follows that the 'integral' scale determined from the zero-frequency intercept of the spectrum is a questionable parameter for defining a typical scale for large eddies. The value of $0.25\ \delta$ will nevertheless be used here because it underestimates the turbulent timescale and should therefore lead to pessimistic conclusions. The inequalities (2), (4), (5), (7) and (8) were evaluated along two streamlines initially located at $y/\delta = 0.1$ and 0.3. The value of $q' \cdot L_d/U \cdot \Lambda$ along both streamlines is less than 0.2 and therefore inequality (2) is satisfied.

The level of dissipation was estimated using a lengthscale Λ_ϵ. This scale is evaluated from the dissipation scale defined by Bradshaw & Ferriss (1971) and along the two streamlines; the ratio $qL_d/(\Delta U \Lambda_\epsilon)$ was about 0.2 and 0.1 respectively. Hence, the dissipation is much less than the production, and inequality (4) is satisfied.

The inequalities resulting from longitudinal diffusion are more questionable: the left-hand side of (5*a*) is approximately 0.2, but the left-hand side of (5*b*) is about 0.4. This inequality resulted from the assumption of negligible turbulence downstream of the expansion, and this very severe condition was not obeyed in our case. Another estimate for the importance of the diffusion may be made by assuming that the longitudinal diffusion term is of order $(\widetilde{u'^2})^{\frac{3}{2}}/L_d$ and by evaluating the numerator from experimental data. By doing so, it is found that the diffusion term is only about 15 % of the production term.

As for the terms in the pressure equation, we can evaluate the frequency limit above which the proposed approximation is valid; in our particular case inequalities (7) and (8) imply that frequency n must be higher than 10 kHz. This frequency is in the energy-containing range, but the main part of the energy occurs at higher frequencies.

In summary, it seems that the inequalities are at last approximately satisfied; the expansion can be considered as a rapid distortion and the simplifications proposed in (II) of (3) can be applied.

Before proceeding to the results of the proposed analysis, it is useful to describe the flow behaviour in terms of the 'extra' rates of strain. The different components of the velocity gradient along the streamline $Q^* = 0.063$ were calculated in an intrinsic frame of reference. The method of characteristics was used to calculate the radii of curvature and the velocity derivatives. As in the expansion studied by Gaviglio *et al.* (1977), the transverse profiles were flattened because of the strong (and inhomogeneous) acceleration. The transverse velocity gradient was reduced to nearly zero and, as a consequence, the mean velocity divergence was much greater than the transverse velocity gradient; typically, the mean divergence was 1.5 times as large as the initial mean shear $(\partial\tilde{u}_1/\partial x_2)_0$. The extra rate of strain due to longitudinal curvature $\partial\tilde{u}_2/\partial x_1$, although it was smaller than $(\partial\tilde{u}_1/\partial x_2)_0$, reached significant negative values. Typically, $D_{12} \approx -0.3\ (\partial\tilde{u}_1/\partial x_2)_0$ and it can therefore be expected to reduce the kinetic energy. The mean rotation rate is not so strongly affected and a 30 % decrease was observed. The rotation rate can change the Reynolds stresses, but it does not affect the kinetic energy.

To evaluate the significance of the bulk dilatation, it was assumed that dilatation effects are the only ones to be taken into account, and consequently that T_{11} is constant. The result, given in figures 8 and 9, shows that dilatation gives the right trend and there is good agreement with experimental data for $y/\delta_0 > 0.4$. Near the wall, however, the observed decrease is not reproduced well by dilatation alone. Note that the initial $\widetilde{u_1'^2}$ profile, for $y/\delta_0 < 0.3$, was not measured but extrapolated on the basis of Klebanoff's data (1954).

The effect of dissipation near the wall was determined in the following way. It was assumed, for $y/\delta_0 < 0.3$, that production balances dissipation in the upstream section, and that the dissipation remains constant in the disturbed zone; this evaluation probably overestimates ϵ. The additional effect on $\widetilde{u_1'^2}$ is given in figure 8, which demonstrates that the dissipation is not of the right magnitude to explain the near-wall behaviour, and can be neglected to a first approximation.

Finally, the complete linear approximation, including all production and pressure contributions (equation (13)) was used to determine $\widetilde{u_1'^2}$ along the streamline $Q^* = 0.063$. The set of equations (13) was written in an intrinsic frame of reference, related to the considered streamline, and the initial values chosen for the different Reynolds stress component correspond to a subsonic self-similar boundary layer, i.e. $\widetilde{u_2'^2} \approx 0.4\widetilde{u_1'^2}$, $\widetilde{u_3'^2} \approx 0.67\widetilde{u_1'^2}$, $\widetilde{u_1'u_2'} = -0.3\widetilde{u_1'^2}$. Figures 8 and 9 show that the complete linear calculation appears to be in better agreement with the measurements than the bulk dilatation approximation. It is striking, however, that the three models for π_{ij} give nearly the same results. In our particular case, however, the contribution of the deviatoric part $D_{ij}+R_{ij}$ compared to the mean pressure gradient terms is rather weak. Although the mean normal strains, the mean shear and the mean rotation rates can all have significant effects, the net result in the expansion is that they do not contribute much to the change in $\widetilde{u_1'^2}$: the dominant term in (13) is the one containing the mean pressure gradient. It is not clear that this result applies for the entire extent of the boundary-layer thickness. On the one hand, it was suggested by Gaviglio *et al.* (1977) that the ratio of the production terms involving dilatation and mean pressure gradient is proportional to $1/M^2$. Therefore, close to the wall, the relative influence of the production terms involving the pressure gradient probably becomes much weaker than at $y/\delta_0 = 0.3$. On the other hand, the mean strain and rotation rate can also change significantly through the vicinity of the wall and the increase of streamline curvature. This could probably contribute to the important decrease of $\widetilde{u_1'^2}$ for $0.1 < y/\delta < 0.3$.

Another interesting result can be deduced. The calculations indicate a considerable change in the turbulence anisotropy; for example, the ratio $\widetilde{u_1'u_2'}.\widetilde{u_{10}'^2}/(\widetilde{u_1'u_2'})_0\widetilde{u_1'^2}$ is about 0.5 and the correlation coefficient R_{12} is reduced by a factor of 2. Unfortunately, these quantities could not be measured in the present experiment. However, at $\delta = 31.3$ mm, the experimental value of $\widetilde{u_1'u_2'}/\widetilde{u_1'^2}$ is nearly -1, for $y/\delta < 0.5$. This result can be due to any of the following reasons.

(i) The experimental determination of $\widetilde{u_1'u_2'}$ from the momentum equation is not very accurate. It may be supposed, from figure 13, that the friction is overestimated by the momentum balance. In addition, the errors in the hot-wire measurements generally lead to an underestimate of the value of $\widetilde{u_1'^2}$ and as a result the error in $\widetilde{u_1'u_2'}/\widetilde{u_1'^2}$ can be about 40 %.

(ii) The models used can be questioned. Very often, different components of the Reynolds stress tensor are not predicted with the same degree of accuracy. In our case, it was found that $\widetilde{u_1'u_2'}$ was very sensitive to the value given to $\alpha(2) = R_{T2}/R_{12}$, which was derived from other work and not checked in our experiment.

(iii) The comparison was made at a station located $2\delta_0$ downstream of the root of the expansion fan. Here the diffusion, dissipation and return to isotropy process can probably no longer be neglected, so that the comparison is probably no longer adequate. A linear calculation, using the LRR model and assuming that only the mean shear is important, indicates that $-\widetilde{u_1'u_2'}$ increases much faster than $\widetilde{u_1'^2}$ downstream of the expansion zone.

6. Conclusion

The rapid distortion of turbulence by a compressible mean flow has been considered with particular application to a solenoidal field of velocity fluctuations subjected to a bulk dilatation. An analysis of the Reynolds stress evolution suggested a modification to the rapid part of the pressure-strain correlation terms for compressible flows. In addition, a new variable was defined which included the explicit effects of density variations, and which can be modelled as the Reynolds stress in subsonic flows with weak inhomogeneities and a weak dissipation rate. The validity of the assumptions was checked in the rapid expansion of a boundary layer in supersonic flow, and the experimental results were in satisfactory agreement with the analysis. Downstream of the expansion the boundary layer begins to recover a new equilibrium state. For example, about ten boundary thicknesses downstream of the distortion a new logarithmic zone appears in the mean velocity profiles. In the external part the turbulence is slowly damped whereas near the wall, at the edge of the 'relaminarized' sublayer which was stabilized by the expansion, the r.m.s. level of velocity increases. This new turbulence gradually invades the remainder of the layer.

In the expansion itself, the Reynolds stress evolution seems to depend mainly on the bulk dilatation production rate and, to a lesser extent, on the mean pressure gradient production, although these latter terms can change the turbulence anisotropy. The magnitude of the terms involving the mean pressure gradient and the turbulent mass flux increases as M^2 and therefore they may play a predominant role in distortions at higher Mach numbers. More refined formulations or empirical information may then be needed to represent these terms. Finally, whatever the generality of the models used in the present work, it seems that a good description of a distortion such as a sudden expansion of a supersonic flow is obtained by assuming that the velocity fluctuations are solenoidal.

The authors are indebted to Professor Bradshaw and Professor Smits for stimulating discussions and suggestions and to Professor Fernholz, Professor Antonia and Dr Debieve for valuable comments; the assistance of Dr Bestion with measurements of spectra and of Dr Delery with the perfect fluid computation is gratefully acknowledged. This work was supported by an ONERA/IMST research contract.

Appendix A. Order-of-magnitude analysis: The Reynolds stress equation

We assume that typical values of velocity and density changes are ΔU and $\Delta\rho$, respectively. U, ρ are representative values of the average velocity and density in the distortion. A scale describing the length of the distortion is L_d and it is assumed that L_d is a significant scale for the mean velocity and mean density variation.

In the case of accelerated flows, we are interested in strong longitudinal gradients, so it will be assumed that $\partial\tilde{u}_1/\partial x_1 \approx \partial\tilde{u}_k/\partial x_k \approx \Delta U/L_d$, and that, outside the viscous sublayer, $|\partial\bar{p}/\partial x_1| \approx \rho U\,\Delta U/L_d$.

As for the velocity fluctuations, it will be supposed that the Reynolds stress anisotropy is not too strong so that $\widetilde{u_1'u_j'} \approx \widetilde{u_k'u_k'} = q'^2$. The instantaneous density fluctuation ρ' is given approximately by formula (1)

$$\frac{\rho'}{\rho} \approx (\gamma-1)\, M^2 \frac{q'}{U},$$

since the correlation coefficient between density and velocity is of order 1. In addition, it is assumed that the turbulent lengthscales for velocity and density fluctuations are nearly the same. Since we are interested in the low wavenumber, energetic range of the spectra, a typical lengthscale Λ is given by the integral scale deduced from two-point correlation measurements.

This scale can be used to estimate the energy dissipation rate $\epsilon \approx q'^3/\Lambda$. However, the order of magnitude of ϵ can be found from the work of Bradshaw & Ferriss (1971), who suggest $\epsilon \approx (-\overline{u_1'u_2'})^{\frac{3}{2}}/L_\epsilon$, where L_ϵ is a dissipation lengthscale and the ratio L_ϵ/δ is assumed to be function of y/δ for equilibrium boundary layers. A dissipation scale Λ_ϵ was deduced from L_ϵ. Hence,

$$-\widetilde{u_1'u_k'}\frac{\partial \tilde{u}_j}{\partial x_k} - \widetilde{u_j'u_k'}\frac{\partial \tilde{u}_j}{\partial x_k} \approx q'^2 \frac{\Delta U}{L_\mathrm{d}}, \tag{I}$$

$$\overline{\frac{\rho' u_1'}{\bar{\rho}^2}}\frac{\partial \bar{p}}{\partial x_j} + \overline{\frac{\rho' u_j'}{\bar{\rho}^2}}\frac{\partial \bar{p}}{\partial x_i} \approx (\gamma-1) M^2 q'^2 \frac{\Delta U}{L_\mathrm{d}}, \tag{II}$$

$$\epsilon_{ij} = \epsilon\, \delta_{ij} \approx \frac{q'^3}{\Lambda_\epsilon}\delta_{ij}. \tag{V}$$

It is more difficult to obtain an estimate of diffusion terms (IV). By assuming that viscous diffusion can neglected, and that $\overline{\rho u_i'u_j'u_k'} \approx \bar{\rho}\ \overline{u_i'u_j'u_k'} \approx \bar{\rho}\ q'^3$, we find that $(1/\bar{\rho})\ (\partial/\partial x_k)\ (\overline{\rho u_i'u_j'u_k'}) \approx (\partial/\partial x_k)\ (\overline{u_i'u_j'u_k'}) + \overline{u_i'u_j'u_k'}\ (1/\bar{\rho})\ (\partial\bar{\rho}/\partial x_k)$. It could be argued that the diffusion scale is of the order of the integral scale of turbulence. This would lead to $(\partial/\partial x_k)\ \overline{u_i'u_j'u_k'} \approx \overline{q'^2}/\Lambda$, and this term is comparable to the dissipation rate. A much more severe condition would be to assume that in our expanded flow the turbulence is completely damped in the distortion so that $(\partial/\partial x_k)\ \overline{u_i'u_j'u_k'} \approx q'^3/L_\mathrm{d}$. We then find:

$$\frac{\partial}{\partial x_k}\overline{u_i'u_j'u_k'} \approx \frac{q'^3}{L_\mathrm{d}},$$

$$\overline{u_i'u_j'u_k'}\frac{1}{\bar{\rho}}\frac{\partial \bar{\rho}}{\partial x_k} \approx q'^3 \frac{\Delta\rho}{\rho L_\mathrm{d}}.$$

It is clear from these estimates that (I) and (II) are comparable for moderate supersonic Mach number, as noted by Gaviglio *et al.* (1977), and that the dissipation rate is small when compared to (I) if

$$\frac{q'}{\Delta U}\frac{L_\mathrm{d}}{\Lambda} \ll 1.$$

Hence, diffusion is much less than production if $q'/\Delta U$ and $(q'/U)\ (\Delta\rho/\rho) \ll 1$.

Appendix B. Terms in the pressure equation

First, the ratio $|(\partial^2 p'/\partial x_k \partial x_k)/(\partial/\partial x_1\ \ln\bar{\rho}\ \partial p'/\partial x_i)|$ is to be evaluated. By taking the Fourier transform of the two terms, this ratio becomes $k^2/|k_i\ (\partial/\partial x_i)\ \ln$

$\bar{\rho}|$, where k_i are the wavenumber vector components. The Laplacian term is dominant if

$$\frac{k^2}{|k_i\,(\partial/\partial x_i)\,\ln\bar{\rho}|} \gg 1,$$

or, approximately $k \gg |(\partial/\partial x_i)\log\bar{\rho}|$.

By assuming Taylor's hypothesis, a condition on the frequency n is deduced

$$n \gg \frac{U}{2\pi}\left|\frac{\partial}{\partial x_i}\ln\bar{\rho}\right|,$$

with the same approximations given in Appendix A, this becomes

$$n \gg \frac{U}{2\pi}\frac{\Delta\rho}{\rho}\frac{1}{L_d}.$$

Secondly, we consider the term

$$\rho'\left(\frac{\partial\tilde{u}_i}{\partial x_j}\frac{\partial\tilde{u}_j}{\partial x_i} - \frac{1}{\bar{\rho}}\frac{\partial\bar{\rho}}{\partial x_i}\tilde{u}_j\frac{\partial\tilde{u}_i}{\partial x_j}\right).$$

Using the same reasoning as above, we find that the two terms in the brackets are both of order $(\Delta U/L_d)^2$. Indeed, in the case of a pure dilatation, both terms equal $\frac{1}{3}(\mathrm{div}\,\tilde{u})^2$. These terms involve a lower wavenumber than $(\partial\rho'/\partial x_i)\tilde{u}_j\ (\partial\tilde{u}_i/\partial x_j)$, and they can be neglected if

$$\frac{\rho'\left(\dfrac{\partial\tilde{u}_1}{\partial x_j}\dfrac{\partial\tilde{u}_j}{\partial x_i} - \dfrac{1}{\bar{\rho}}\dfrac{\partial\bar{\rho}}{\partial x_i}\tilde{u}_j\dfrac{\partial\tilde{u}_i}{\partial x_j}\right)}{\dfrac{\partial\rho'}{\partial x_i}\tilde{u}_j\dfrac{\partial\tilde{u}_i}{\partial x_j}} \gg 1,$$

i.e.

$$\frac{\Delta U}{k\,UL_d} \ll 1 \quad \text{or} \quad n \gg \frac{\Delta U}{2\pi L_d}.$$

Appendix C.

1. *Diffusion of total enthalpy*

For steady mean flows, the equation for total enthalpy $C_p\tilde{T}_t$ reads

$$\frac{\mathrm{D}}{\mathrm{D}t}\tilde{T}_t = \frac{1}{\bar{\rho}C_p}\frac{\partial}{\partial x_k}\Bigg[\overline{\mu\left(\frac{\partial u_i}{\partial x_k}+\frac{\partial u_k}{\partial x_i}-\frac{2}{3}\frac{\partial u_j}{\partial x_j}\delta_{ik}\right)u_k} - \lambda\overline{\frac{\partial T}{\partial x_k}}$$
$$-C_v\overline{\rho\,u_k'T'} - \tilde{u}_j\overline{\rho\,u_k'u_j'} - \overline{pu_k'} - \frac{1}{2}\overline{\rho u_j'u_j'u_k'}\Bigg],$$

with

$$\tilde{T}_t = \tilde{T} + \frac{\tilde{u}_i\tilde{u}_i}{2C_p} + \frac{\widetilde{u_i'u_i'}}{2C_p}.$$

Outside the viscous sublayer, viscous and heat conduction terms may be ignored. Further, the order of magnitude of the right-hand-side member is assumed to be given by

$$-\frac{1}{C_p}\frac{1}{\bar{\rho}}\frac{\partial}{\partial x_2}(C_v\overline{\rho\,u_2'T'} + \tilde{u}_1\overline{\rho u_{21}''} + \bar{p}\,\overline{u_2'}).$$

Applying the SRA, and neglecting the density gradient, this term is reduced to

$$-\frac{1}{C_p}\frac{\partial}{\partial x_2}\left[\widetilde{u_1'u_2'}\cdot\tilde{u}_1\,(1+R_{vT}/R_{uv})\right];$$

it is of the order of

$$-\frac{1}{C_p}\frac{\partial}{\partial x_2}(\tilde{u}_1\,\overline{u_1'u_2'}).$$

The variation $\Delta\tilde{T}_t$ of total temperature produced after a distance L_d is:

$$\Delta\tilde{T}_t \approx -\int_0^{L_d}\frac{1}{\tilde{u}_1 C_p}\frac{\partial}{\partial x_2}(\tilde{u}_1\,\overline{u_1u_2})\,\mathrm{d}x_1,$$

$$\Delta\tilde{T}_t \approx +\frac{\tau_0}{C_p}\frac{L_d}{\delta},$$

where it was supposed that $\partial(\tilde{u}_1 u_1' u_2')/\partial x_2$ is approximately $U\,\tau_0/\delta$. U is an average value of the mean velocity in the distortion; it is here confused with the local value $\tilde{u}_1$. τ_0 is the friction upstream of the distortion and δ the layer thickness.

2. *Variations of mean entropy in a rapid distortion*

The equation for mean entropy $\tilde{s}$ reads:

$$\bar{\rho}\frac{\mathrm{D}}{\mathrm{D}t}\tilde{s} = \frac{\partial}{\partial x_k}\left(\frac{\lambda}{T}\frac{\partial T}{\partial x_k} - \overline{\rho\,u_k's_k'}\right) + \left(\overline{\frac{\rho\epsilon}{T}}\right) + \left(\overline{\frac{\lambda}{T^2}\frac{\partial T}{\partial x_k}\frac{\partial T}{\partial x_k}}\right).$$

A particular situation is examined: the Reynolds (or Péclet) number is large, so that the dissipation in the mean motion and the conduction by mean temperature can be neglected. Moreover, the fluctuations are supposed small and the 'no sound' assumption is used. Then,

$$\frac{\partial}{\partial x_k}\overline{\rho s'u_k'} \approx \frac{\partial}{\partial x_2}C_p\frac{\overline{\rho\,T'u_2'}}{\tilde{T}} \approx -\frac{\partial}{\partial x_2}\frac{\bar{\rho}}{\tilde{T}}\overline{u_1'u_2'}\,\tilde{U}_1.$$

With the assumption that $\rho'/\bar{\rho} \ll 1$ and $T'/\tilde{T} \ll 1$, after expanding the last two terms on the left of the entropy equation and neglecting density and temperature fluctuations, the following approximation is obtained:

$$\overline{\frac{\rho\epsilon}{T}} \approx \frac{\bar{\rho}}{\tilde{T}}\bar{\epsilon},$$

$$\overline{\frac{\lambda}{T^2}\frac{\partial T}{\partial x_k}\frac{\partial T}{\partial x_k}} \approx \frac{\bar{\lambda}}{\tilde{T}^2}\left(\overline{\frac{\partial T'}{\partial x_k}\frac{\partial T'}{\partial x_k}}\right) = C_v\frac{\bar{\rho}}{\tilde{T}^2}\epsilon_T.$$

If, as in subsonic flows, $\epsilon_T \approx \epsilon(T'^2/q'^2)$, then

$$\frac{C_v\epsilon_T}{\tilde{T}} \approx \frac{(\gamma-1)}{\gamma}M^2\,\epsilon.$$

It follows that, for non-hypersonic Mach numbers, these two terms have comparable values. On the other hand, it is obvious that turbulent diffusion and dissipation are of the same order.

Then a rough but reasonable estimate of the entropy change Δs through the distortion is given by:

$$\Delta s = \int_0^{L_d}\frac{\bar{\epsilon}}{\overline{UT}}\mathrm{d}x_1 \approx \frac{\epsilon}{\overline{UT}}L_d.$$

Since ϵ is nearly constant in the distortion, its value can be taken as that in the initial boundary layer, namely $\epsilon = q_0'^3/\Lambda_0$. Then

$$\Delta s \approx \gamma R \frac{L_d}{\Lambda_0} \frac{q_0'}{U} m_0^2,$$

with

$$m_0 = q_0'/(\gamma RT)^{\frac{1}{2}}.$$

REFERENCES

ALLEN, J. M. 1972 Impact probe displacement in a supersonic turbulent boundary layer. *AIAA J.* **10** (4), 555–556.

BATCHELOR, G. K. 1955 The effective pressure exerted by a gas in turbulent motion. *Vistas in Astronomy* **1**, 290–295.

BATCHELOR, G. K. & PROUDMAN, I. 1954 The effect of rapid distortion of a fluid in turbulent motion. *Q. J. Mech. Appl. Maths.* **7**, 83.

BESTION, D., DEBIÈVE, J. F. & DUSSAUGE, J. P. 1983 Too-rapid distortions in supersonic flows: turbulence-shock wave and turbulence-expansion. Structure of complex turbulent shear flows. *IUTAM symposium, Marseille, 1982* (ed. R. Dumas & L. Fulachier), pp. 289–298. Springer.

BONNET, J. P. & ALZIARY DE ROQUEFORT, T. 1982 Measurement of turbulence correlations in a two-dimensional supersonic wake. *Symp. Heat and Mass Transfer and the Structure of Turbulence, Dubrovnik. 1980.* Hemisphere.

BRADSHAW, P. 1974 The effect of mean compression or dilatation on the turbulence structure of supersonic boundary layers. *J. Fluid Mech.* **63**, 449–464.

BRADSHAW, P. 1976 Complex turbulent flows. In *Theoretical and Applied Mechanics* (ed. W. T. Koiter), pp. 104–113. North-Holland.

BRADSHAW, P. 1977. Compressible turbulent shear layers. *Ann. Rev. Fluid Mech.* **9**, 33–54.

BRADSHAW, P. & FERRISS, D. H. 1971 Calculation of boundary layer development using the turbulent energy equation: compressible flow on adiabatic walls. *J. Fluid Mech.* **46**, 83–110.

CHEW, Y. T. 1978 Two-parameter skin-friction formula for adiabatic compressible flow. *AIAA J.* **16**, 186–188.

CHEW, Y. T. & SQUIRE, L. C. 1979 The boundary layer development downstream of a shock interaction at an expansion corner. *Aeronautical Research Council, R & M* no. 3839. London.

CRAYA, A. 1958 Contribution à l'analyse de la turbulence associée à des vitesses moyennes. *PST no.* 345. Paris: Ministère de l'Air.

DEBIEVE, J. F. 1983 Etude d'une interaction turbulence–onde de choc. Thése d'Etat, Univ. Aix-Marseille II.

DEBIEVE, J. F., GOUIN, M. & GAVIGLIO, J. 1982 Momentum and temperature fluxes in a shock wave turbulence interaction. *Symp. Heat and Mass Transfer and the Structure of Turbulence Dubronik 1980.* Hemisphere.

DÉLERY, J. & MASURE, B. 1969 Action d'une variation brusque de pression sur une couche limite turbulente et application aux prises d'aire hypersoniques. *La Recherche Aérospatiale*, no. 129, pp. 3–12.

DEMETRIADES, A. 1976 Turbulence correlations in a compressible wake. *J. Fluid Mech.* **74**, 251–268.

DUSSAUGE, J. P. 1981 Evolution de transferts turbulents dans une détente rapide en écoulement supersonique. Thèse d'Etat, Univ. Aix-Marseille II.

ELENA, M., BOREL, A. & GAVIGLIO, J. 1977 Interaction couche limite turbulente – Onde de choc – 1: couche limite initiale, dispositif d'expérience. *RT ONERA* 15/1455 AN.

ELENA, M. & GAVIGLIO, J. 1983 Confrontation de mesures par anémomètres à laser et à fil chaud, en couches limites turbulentes, à vitesse supersonique. *Proc. 20th Colloque d'Aérodynamique Appliquée, Toulouse, France, Novembre 8–10.*

FAVRE, A., KOVASZNAY, L. S. G., DUMAS, R., GAVIGLIO, J. & COANTIC, M. 1976 *La Turbulence en Mécanique des Fluides.* Gauthier-Villars.

FEIEREISEN, W. J., REYNOLDS, W. C. & FERZIGER, J. H. 1981 Numerical simulation of a compressible homogeneous turbulent shear flow. *Thermoscience Division Rep. no.* TF-13, Dept. Mech. Engng, Stanford University.

FERNHOLZ, H. H. & FINLEY, P. J. 1980 A critical commentry on mean flow data for two-dimensional compressible boundary layers. *AGARDograph* **253**.

FERNHOLZ, H. H. & FINLEY, P. J. 1981 A further compilation of compressible boundary layer data with a survey of turbulence data. *AGARDograph* **263**.

GALMES, J. M., DUSSAUGE, J. P. & DEKEYSER, I. 1983 Couches limites turbulentes supersoniques soumises à un gradient de pression: calcul à l'aide d'un modèle k–ϵ. *J. Méc.* **2** (4), 539–558.

GAVIGLIO, J. 1971 Sur la détermination des sensibilités des anémothermomètres à fil chaud en écoulement supersonique. *C.R. Acad. Sci. Paris.* A **273**, 634–637.

GAVIGLIO, J. 1978 Sur les méthodes de l'anémomètrie pa fil chaud des écoulements turbulents compressible des gaz. *J. Méc.* **2** (4), 449–498.

GAVIGLIO, J., DUSSAUGE, J. P., DEBIEVE, J. F. & FAVRE, A. 1977 Behavior of a turbulent flow, strongly out of equilibrium, at supersonic speeds. *Phys. Fluids* **20**, 5179–5192.

GAVIGLIO, J. & DUSSAUGE, J. P. 1977 On reduction of errors arising in hot-wire anemometry of thin turbulent shear layers. *National Bureau of Standards Special Publication no.* 484 (ed. L. K. Irwin) and TP ONERA no. 1977-168.

GOLDSTEIN, M. E. 1978 Unsteady vortical and entropic distortions of potential flows round arbitrary obstacles. *J. Fluid Mech.* **89**, 433–468.

GOLDSTEIN, M. E. 1979 Turbulence generated by the interaction of entropy fluctuations with non-uniform mean flows. *J. Fluid Mech.* **93**, 209–224.

HUNT, J. C. R. 1973 A theory of turbulent flow round two-dimensional bluff bodies, *J. Fluid Mech.* **61**, 625–706.

HUNT, J. C. R. 1977 A review of the theory of rapidly distorted turbulent flows and its applications. *Fluid Dynamics Transaction*, vol. 9, pp. 121–152. Thirteenth Biennial Fluid Dynamics Symposium, Poland.

JOHNSON, D. A. & ROSE, W. C. 1975 Laser velocimeter and hot-wire anemometer comparison in a supersonic boundary layer. *AIAA J.* **13**, 512–515.

KISTLER, A. L. 1959 Fluctuations measurements in a supersonic turbulent boundary layer. *Phys. Fluids* **2**, 290–296.

KLEBANOFF, P. S. 1954 Characteristics of turbulence in a boundary layer with zero pressure gradient. *NACA TN* 3178. Washington, DC.

KOVASZNAY, L. S. G. 1953 Turbulence in supersonic flow. *J. Aero. Sci.* **20**, 657–675.

LAUFER, J. 1969 Thoughts on compressible turbulent boundary layers. *The RAND Corp., Memo RM, 5946 PR.* University of California.

LAUFER, J. & MCCLELLAN, R 1956 Measurements of heat transfer from fine wires in supersonic flows. *J. Fluid Mech.* **1**, 276–289.

LAUNDER, B. E., REECE, G. J. & RODI, W. 1975 Progress in the development of a Reynolds stress turbulent closure. *J. Fluid. Mech.* **68**, 537–566.

LUMLEY, J. L. 1975 Prediction methods for turbulent flows introduction. Institut von Kármán, Rhodes-Saint-Genèse, Belgium.

MICHEL, R. 1960 Résultats sur la couche limite turbulente aux grandes vitesses. Tenth Congrès de Mécanique Appliquée, Stresa. *ONERA no.* 102.

MOFFATT, H. K. 1968 The interaction of turbulence with a strong wind shear. *International Colloquium on Atmospheric Turbulence and Radio Wave Propagation, Moscow 1965* (ed. Y. Yaglom & V. I. Tatarsky), pp. 139–150. Moscow: Nauka.

MORKOVIN, M. V. 1955 Effects of high acceleration on a turbulent supersonic shear layer. Heat Transfer and Fluid Mechanics Institute, Stanford University.

MORKOVIN, M. V. 1962 Effects of compressibility on turbulent flows. *Mécanique de la Turbulence* (ed. A. Favre), pp. 367–380. CNRS.

MOYAL, J. E. 1952 The spectra of turbulence in a compressible fluid: eddy turbulence and random noise. *Proc. Camb. Phil. Soc.* **48**, 329.

NAOT, D., SHAVIT, A. & WOLFSTHEIN, M. 1970 Interaction between components of the turbulent velocity correlation tensor due to pressure fluctuations. *Israel J. Tech.* **8**, 259.

NARASIMHA, R. & SREENIVASAN, K. R. 1979 Relaminarization of fluid flows. *Adv. Appl. Mech.* **19**, 221–309.

NARASIMHA, R. & VISWANATH, P. R. 1975 Reverse transition on expansion corner in supersonic flows. *AIAA J.* **13**, 693–695.

RIBNER, H. S. & TUCKER, M. 1952 Spectrum of turbulence in a contracting stream. *NACA TN* 2606. Washington.

RUBESIN, M. W. 1976 A one-equation model of turbulence for use with the compressible Navier–Stokes equations. *NASA TM* X-73, 128.

SABOT, J., RENAULT, J. & COMTE-BELLOT, G. 1973 Space–time correlations of the transverse velocity fluctuation in pipe-flow. *Phys. Fluids.* **16**, 1403–1405.

SMITS, A. J., HAYAKAWA, K. & MUCK, K. C. 1983 Constant temperature hot-wire anemometer practice in supersonic flows. *Exp. Fluids* **1**, 83–92.

SMITS, A. J. & WOOD, D. H. 1985 The response of turbulent boundary layer to sudden perturbations. *Ann. Rev. Fluid Mech.* **17**, 321–358.

STERNBERG, J. 1954 The transition from a turbulent to a laminar boundary layer. Aberdeen Proving Group, Ballistic Research Lab. MD, USA.

TOWNSEND, A. A. 1980 The response of a sheared turbulence to additional distortion. *J. Fluid Mech.* **98**, 171–192.

VOISINET, R. L. P. & LEE, R. E. 1972 Measurements of a Mach 4.9 zero pressure gradient turbulent boundary layer with heat transfer. *NOLTR* 72–232.

WILCOX, D. C. & ALBER, I. E. 1972 A turbulence model for high speed flows. Heat Transfer and Fluid Mechanics Institute, Stanford University, Stanford, California.

WILCOX, D. C. & RUBESIN, M. W. 1980 Progress in turbulence modeling for complex flow field including effects of compressibility. *NASA TR* 1517.

YANTA, W. J. & CRAPO, B. J. 1976 Laser velocimetry applied to transsonic and supersonic aerodynamics. Application of non-intrusive instrumentation in fluid flow-research. *AGARD Conf. Proc.* **193**.

YOUNG, A. D. 1951 The equations of motion and energy and the velocity profile of a turbulent boundary layer in a compressible fluid. *College of Aeronautics, Cranfield, England, Rep.* no. 42. 42.